



**The Abdus Salam
International Centre for Theoretical Physics**



2272-3

**Joint ICTP-IAEA School on Synchrotron Applications in Cultural Heritage and
Environmental Sciences and Multidisciplinary Aspects of Imaging Techniques**

21 - 25 November 2011

**X-ray Microscopy and X-ray Fluorescence: applications in cultural heritage and
environmental sciences**

Alessandra Gianoncelli
*Elettra, Trieste
Italy*



TwinMic

<http://www.elettra.trieste.it/twinmic>
The twin X-ray microscopy station at ELETTRA



X-ray Microscopy and X-ray Fluorescence: applications in cultural heritage and environmental sciences

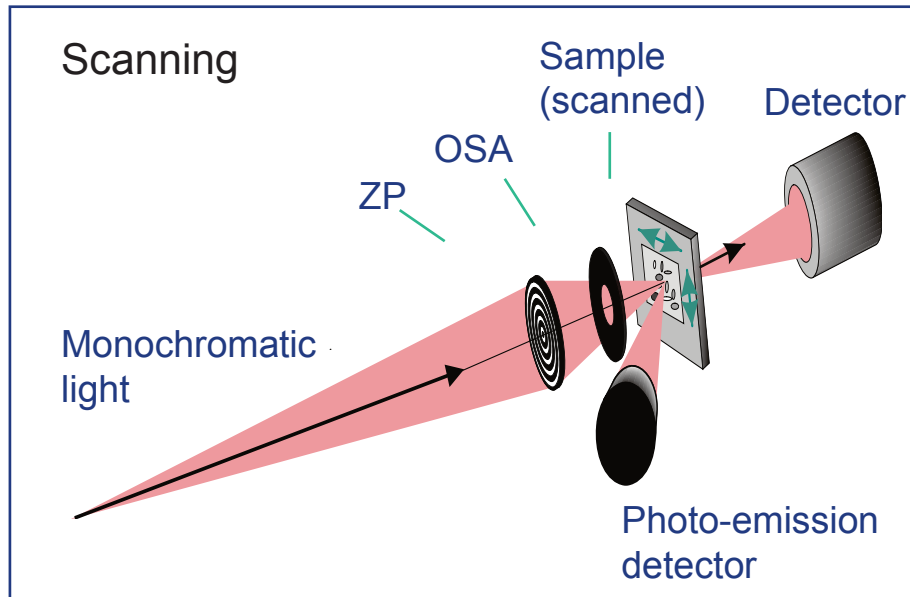
Alessandra Gianoncelli



ELETTRA – Sincrotrone Trieste

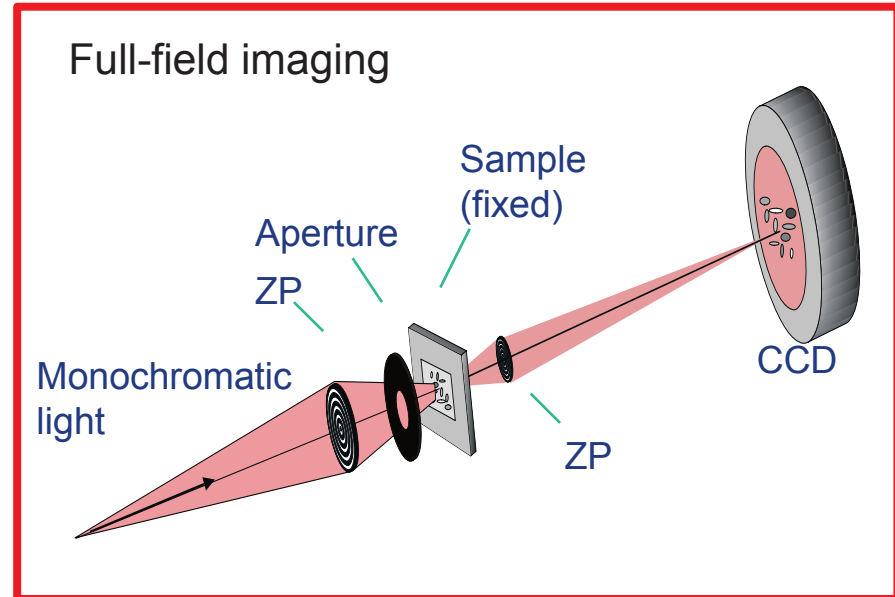
alessandra.gianoncelli@elettra.trieste.it

Background info: X-ray microscopy types



- + versatile detectors can run simultaneously;
- + easier optics set-up;
- long exposure time;
- complex electronics.

Ideal for spectromicroscopy

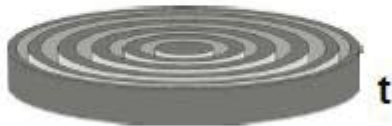


- + short exposure time;
- + higher resolution
- static system;
- complex optical alignment.

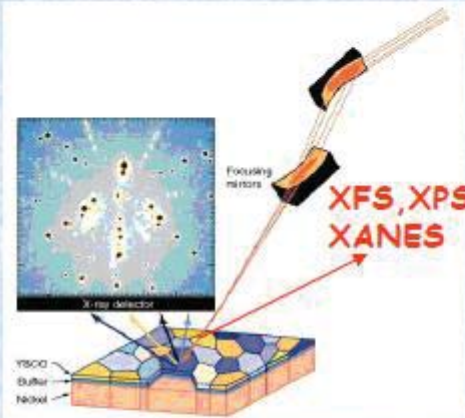
Ideal for dynamic studies
and tomography



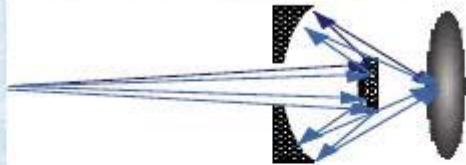
Focusing optics: zone plates, mirrors, capillaries



Zone Plate optics: from ~
200 to ~ 8000 eV
Resolution: 30 nm in
transmission

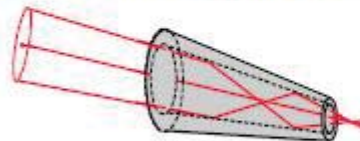


KP-B mirrors each
focusing in one direction:
soft & hard: ~ 1000 nm
Soft & hard x-rays!
chromatic focal point,
easy energy tunability,
comfortable working
distance
Resolution ~ 1000 nm



Normal incidence:
spherical mirrors with
multilayer interference coating
(Schwarzschild Objective)
not tunable, $E < 100$ eV
Resolution: best ~ 100 nm

Capillary: multiple
reflection concentrator



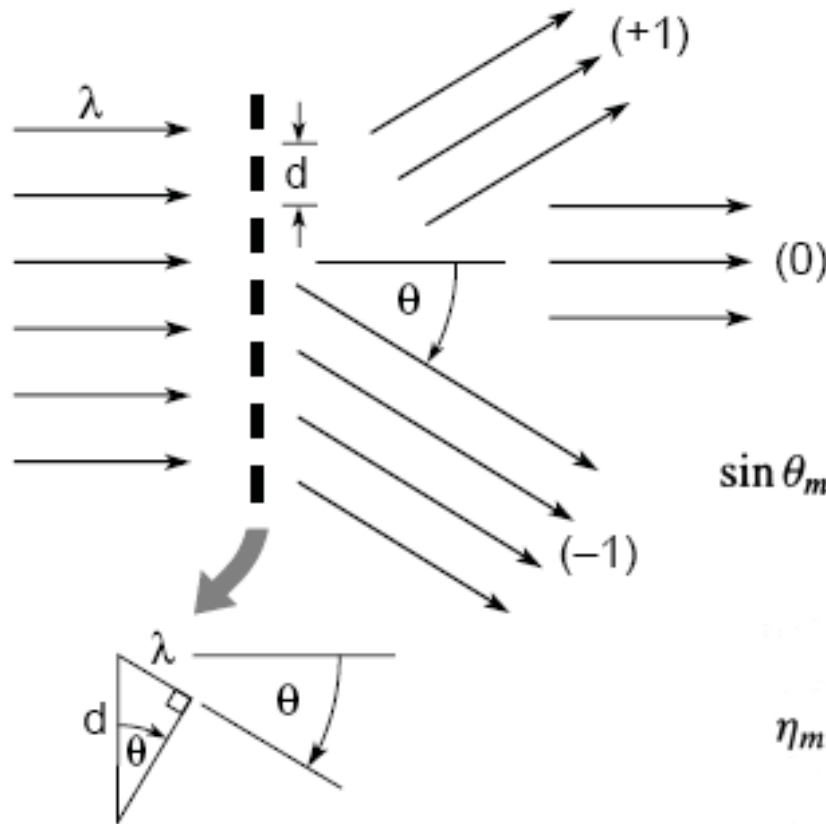
Hard x-rays ~ 8-18 keV
Resolution: > 3000 nm

Refractive lenses



Hard x-rays ~ 4-70 keV
Resolution: > 1000 nm

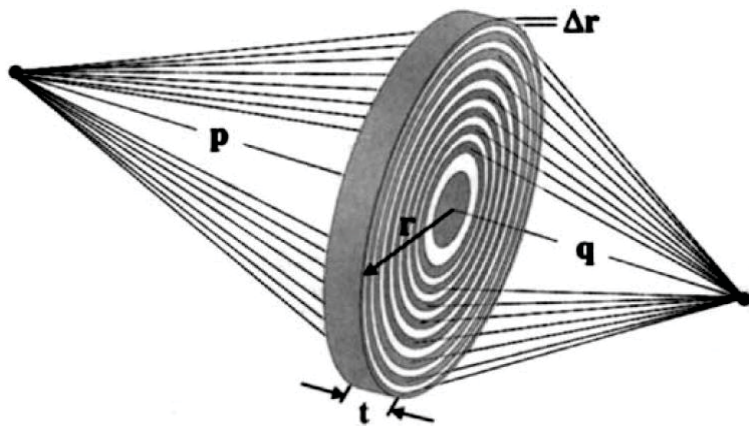
Background info: Diffraction by a grating



$$\sin \theta_m = \frac{m\lambda}{d} ; \quad m = 0, \pm 1, \pm 2, \pm 3, \dots \quad (9.2)$$

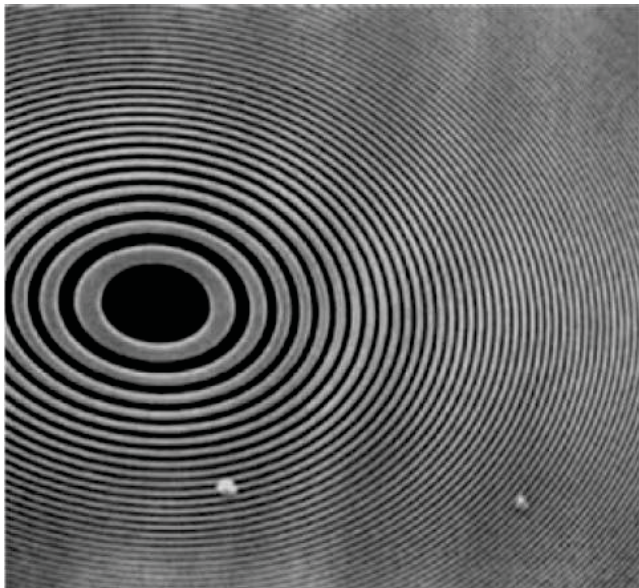
$$\eta_m = \begin{cases} \frac{1}{4} & m = 0 \\ 1/m^2\pi^2 & m \text{ odd} \\ 0 & m \text{ even} \end{cases} \quad (9.24)$$

(50% absorbed)



Zone plate (ZP) is a circular diffraction grating with radially increasing line density

$$\frac{1}{f} = \frac{1}{p} + \frac{1}{q} \quad \text{if } n > 100; \quad f = \frac{2r\Delta r}{\lambda}$$



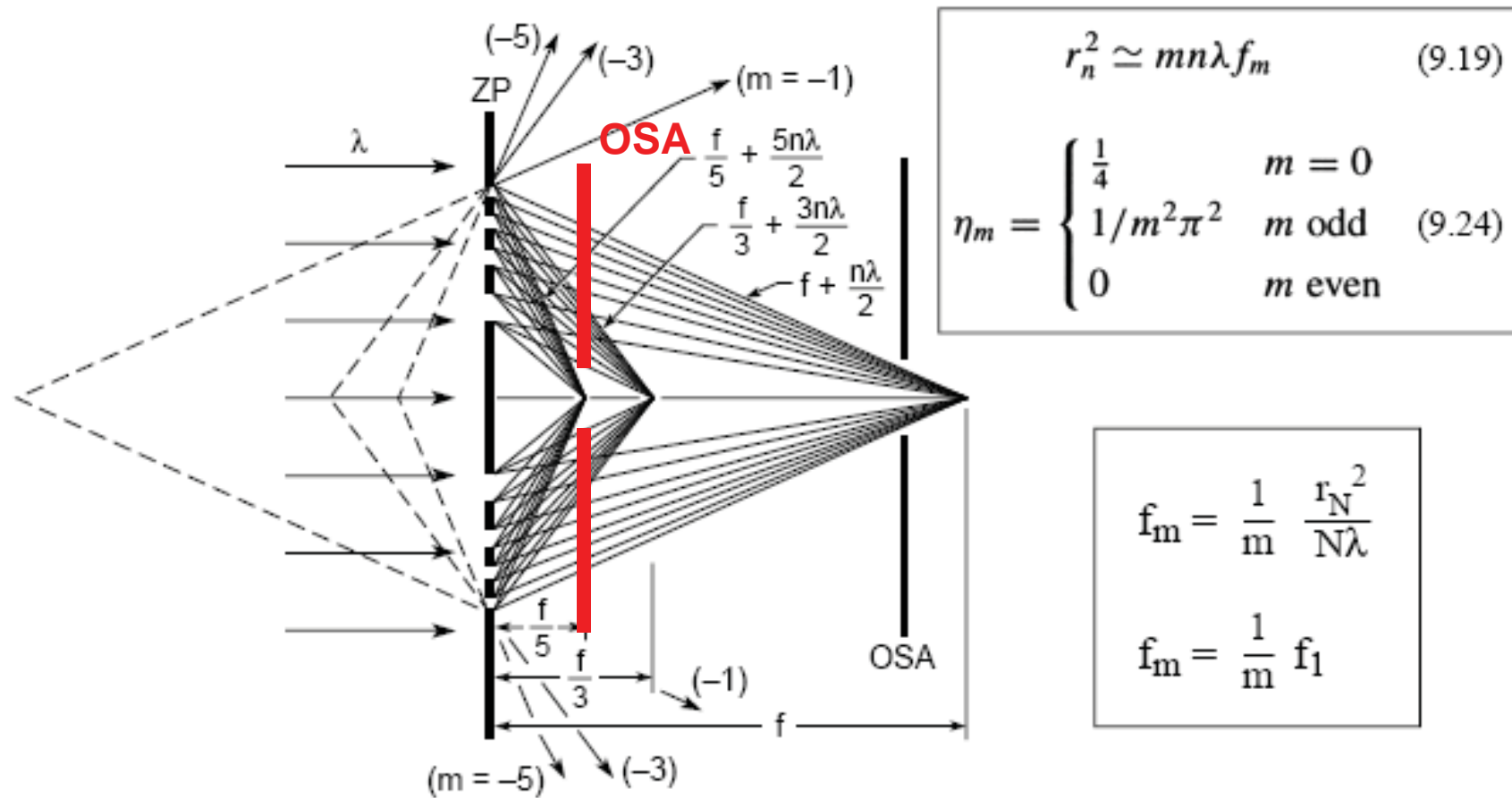
Lateral resolution of a ZP (Rayleigh):

$$NA \equiv \frac{r}{f} = \frac{\lambda}{2\Delta r}$$

$$\delta_{Rayleigh} = \frac{0.61\lambda}{NA} = 1.22\Delta r$$

(not smaller than the diffraction limit of the wavelength)

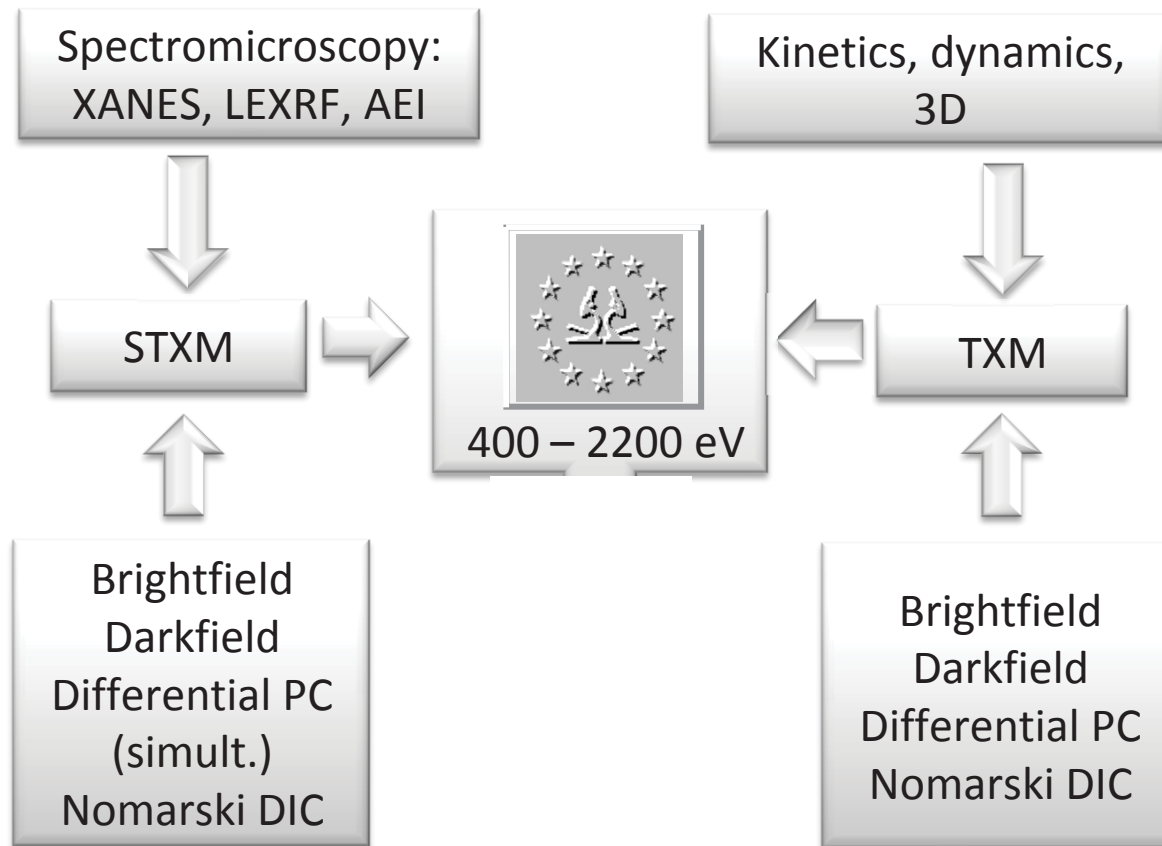
Background info: Diffraction by a grating





The TwinMic microscope at ELETTRA

Integrating both modes into a *single* instrument?

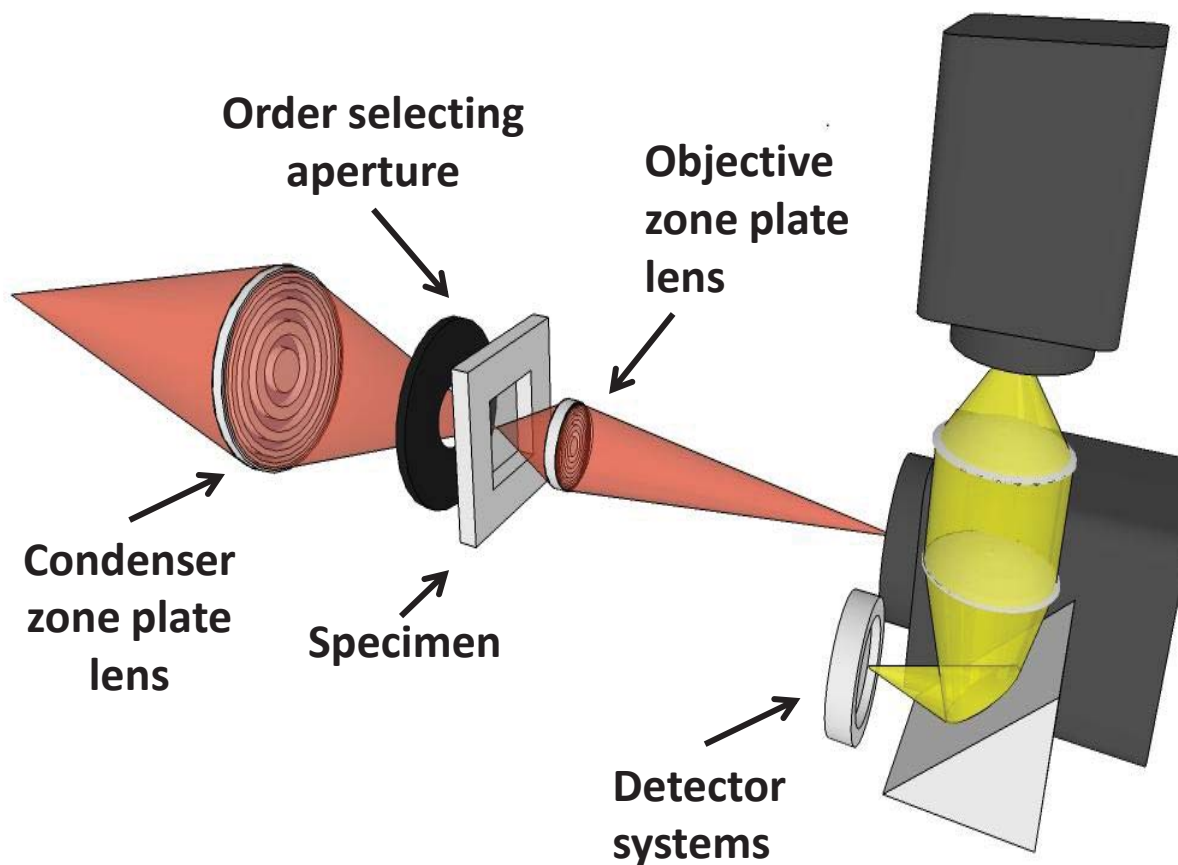


- Biotechnology
- Nanotechnology
- Environment
- Geochemistry
- Food Science
- Medicine
- Pharmacology
- Cultural Heritage
- New Materials



Imaging modes in X-ray microscopy

The full-field imaging mode

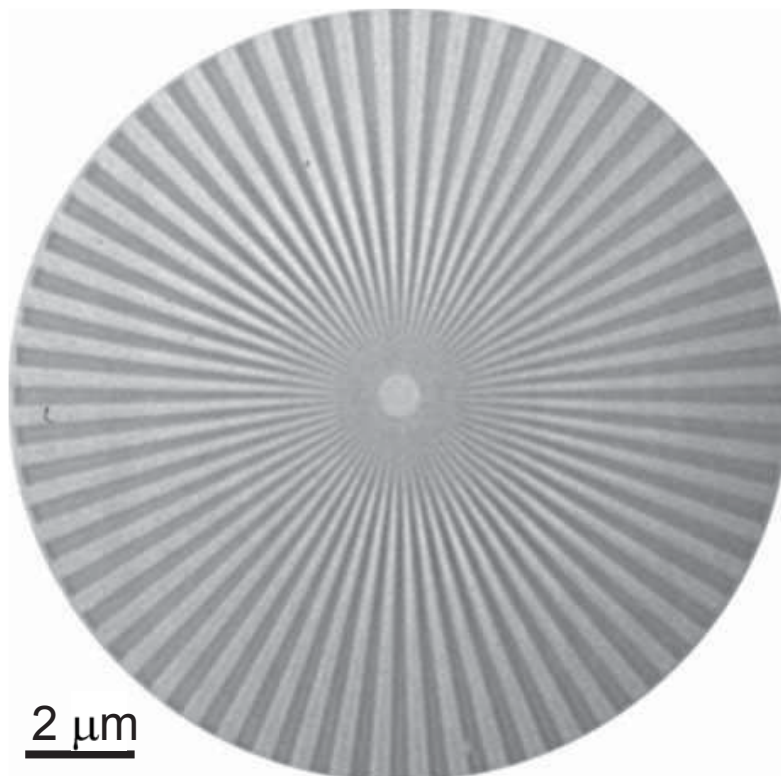


Gunther Schmahl

- Similar to conventional visible light microscope
- Analysis of morphology in transmission
- Fast imaging, dynamics, microtomography



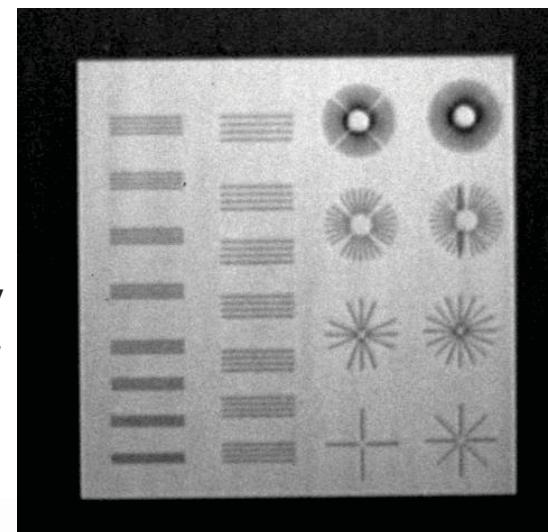
Resolution tests of a ZP



2 μm

*Experiment performed by
M. Prasciolu and D. Cojoc, TASC/ INFM)*

ZP parameters:
110 μm diameter
50 nm outer zones
f=3.2 mm @ 720 eV
fabricated by TASC/
INFM



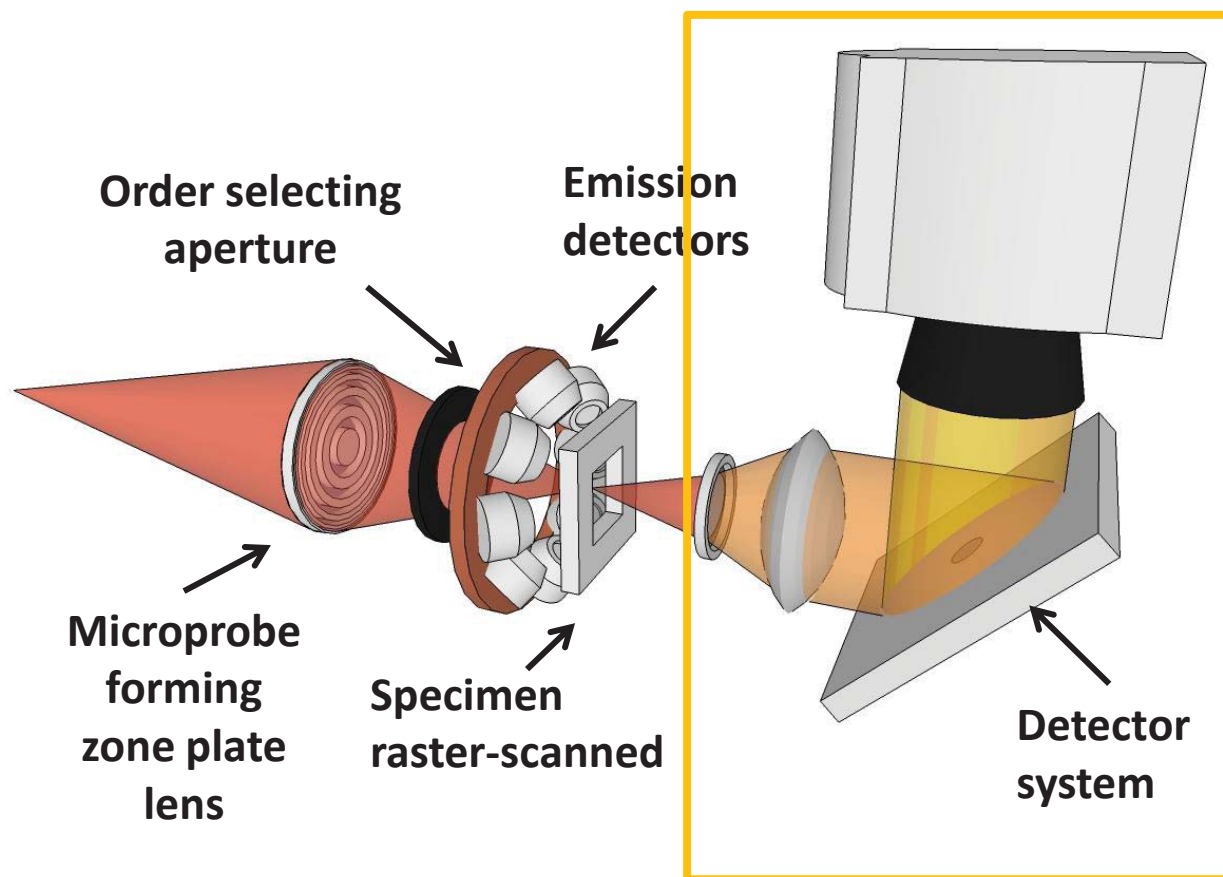
2 μm

Test pattern with
30 nm features
(fabricated by
TASC/ INFM)



Imaging modes in X-ray microscopy

The scanning transmission and emission mode



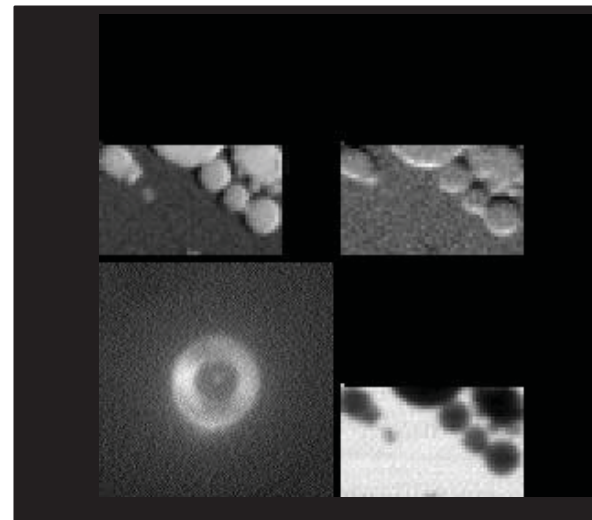
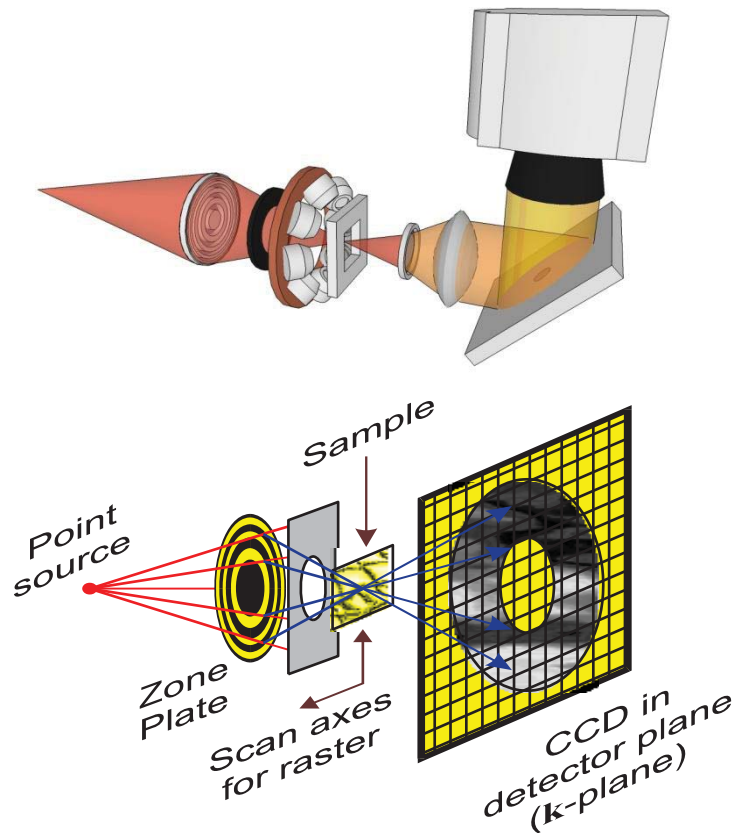
Janos Kirz

- Simultaneous acquisition of different transmission and emission signals
- Elemental mapping and chemical analysis
- Slower and more complex data acquisition



Scanning transmission mode

Differential phase contrast with a fast read-out CCD camera



Simultaneous acquisition of:

- Absorption or transmission
- Differential phase contrast
- Darkfield images

Optics based:

- Zernike phase contrast (Schmahl et al.)
- Differential interference contrast (Wilhein et al., Kaulich et al.)

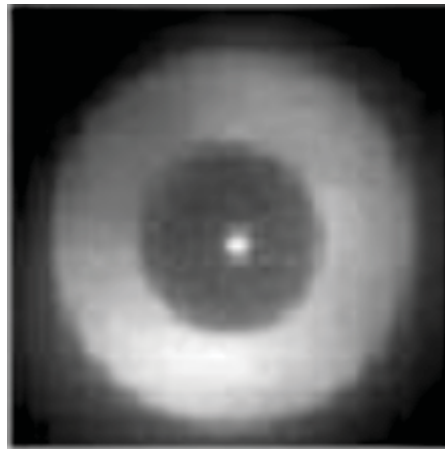
Detector based:

- Differential phase contrast (Morrison et al.,

Feser et al.,
Hornberger et al.

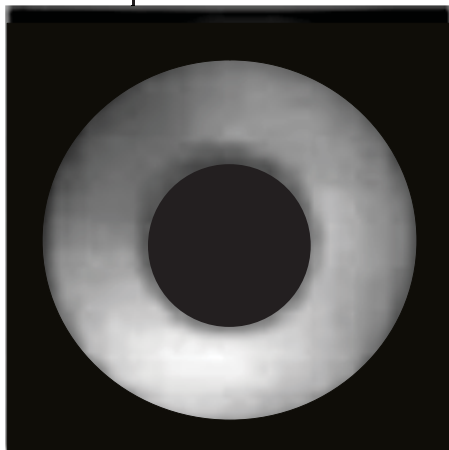


Computational extraction of contrasts by masking:

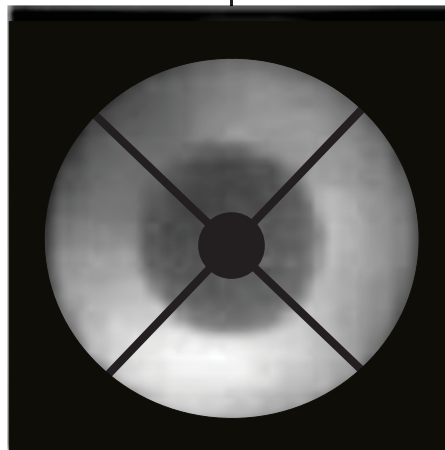


Raw data acquisition of first diffraction order image for each pixel of the raster scan

Applying different masks



Bright field

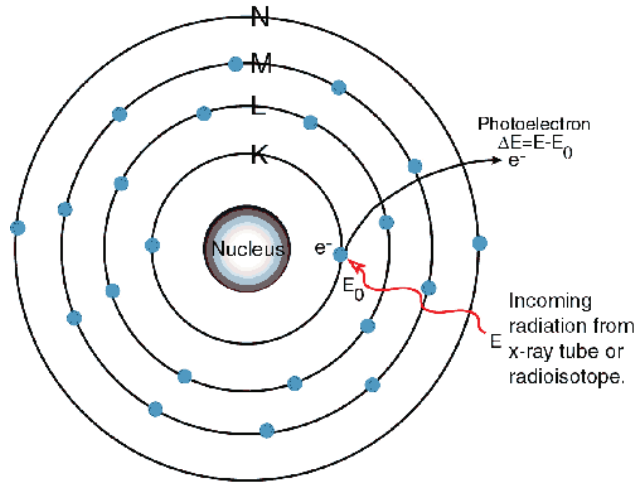


Differential phase and absorption



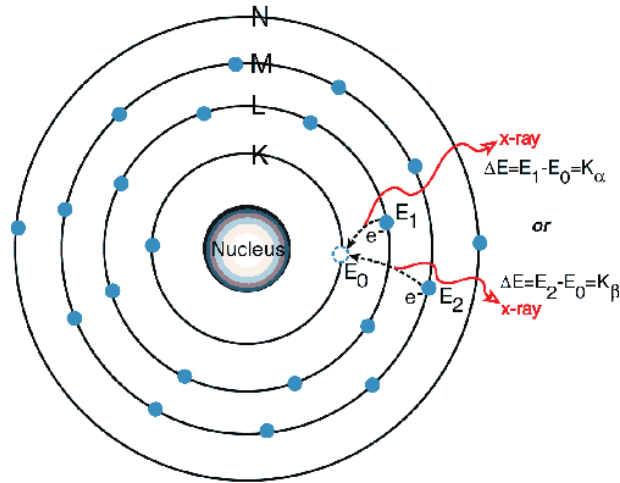
Darkfield

Photoionization



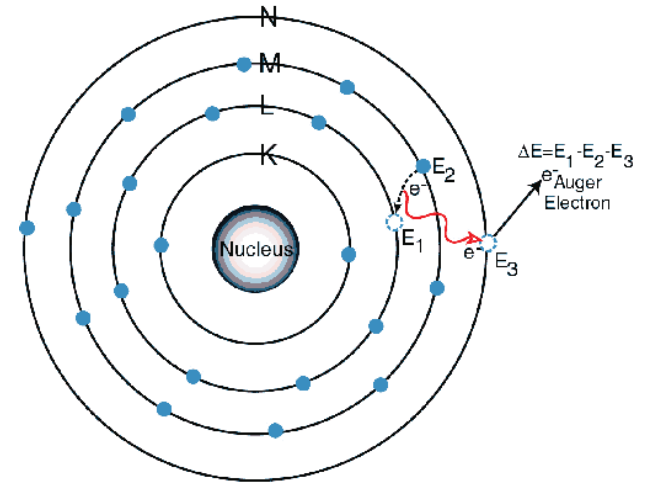
X-ray absorption
(through photoelectric effect)

The primary X-ray photon causes the ejection of electrons from the inner shells, creating vacancies



X-ray Fluorescence

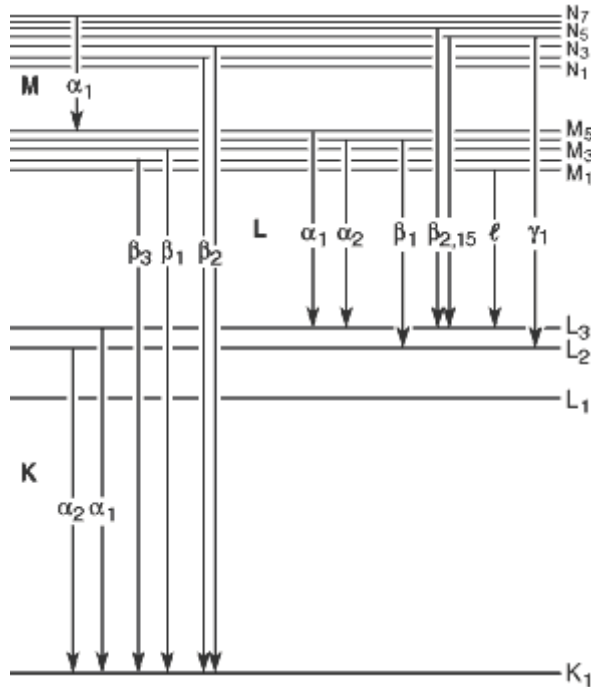
The vacancy created by the primary X-ray photon is filled by an electron coming from an outer shell causing the emission of a characteristic X-ray photon whose energy is the difference between the two binding energies of the corresponding shells



Auger effect

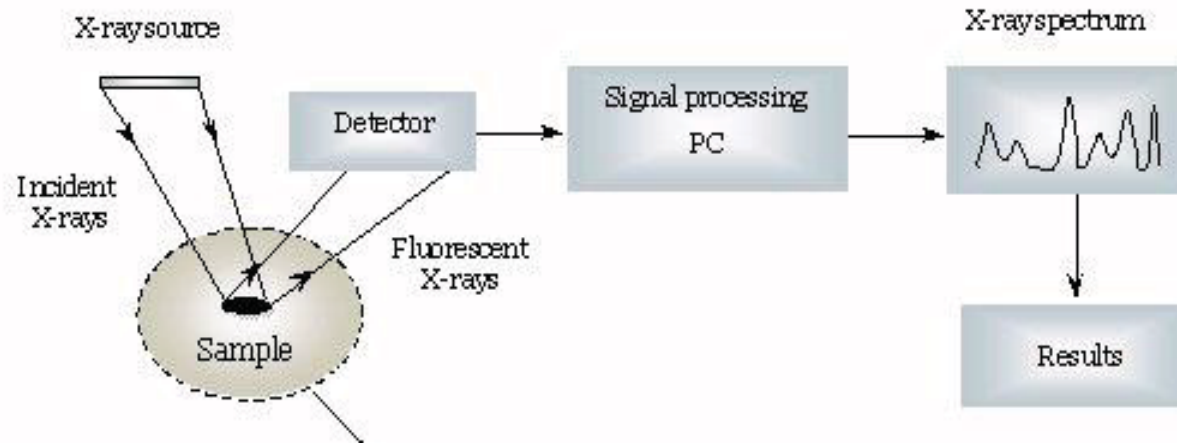
The vacancy created by the primary X-ray photon is filled by an electron coming from an outer shell and the energy is transferred directly to one of the outer electrons, causing it to be ejected from the atom.

X-ray Fluorescence (XRF)



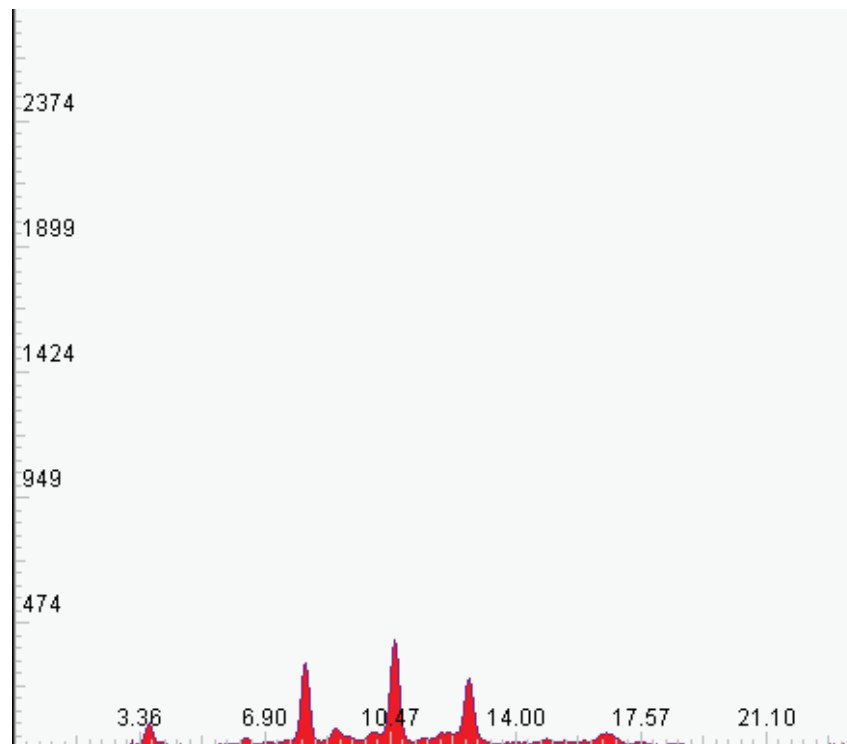
- **X-ray fluorescence (XRF)** is the phenomenon where an electron from an outer shell then drops into the unoccupied orbital, to fill the hole left behind. This transition gives off an X-ray of fixed, characteristic energy that can be detected by a fluorescence detector.
 - The energy needed to eject a core electron is **characteristic of each element**, and so is the energy emitted by the transition. The transition of an L shell electron dropping into the K shell is termed a K α transition, while an M shell electron dropping into the K shell is a K β transition.
- Elemental analysis technique
 - Non destructive (no sample preparation, in air, no damages on the sample)
 - Analysis of the surface sample layers (the XRF photons must be able to exit the sample and reach the detector)

XRF system



- Source: X-rays
 - Detector: solide state (Ge, Si), photomultiplier
 - Signal processing: preamplifier + filter shaping + multichannel analyser
 - PC + analysis software (qualitative and quantitative)
-

XRF spectrum

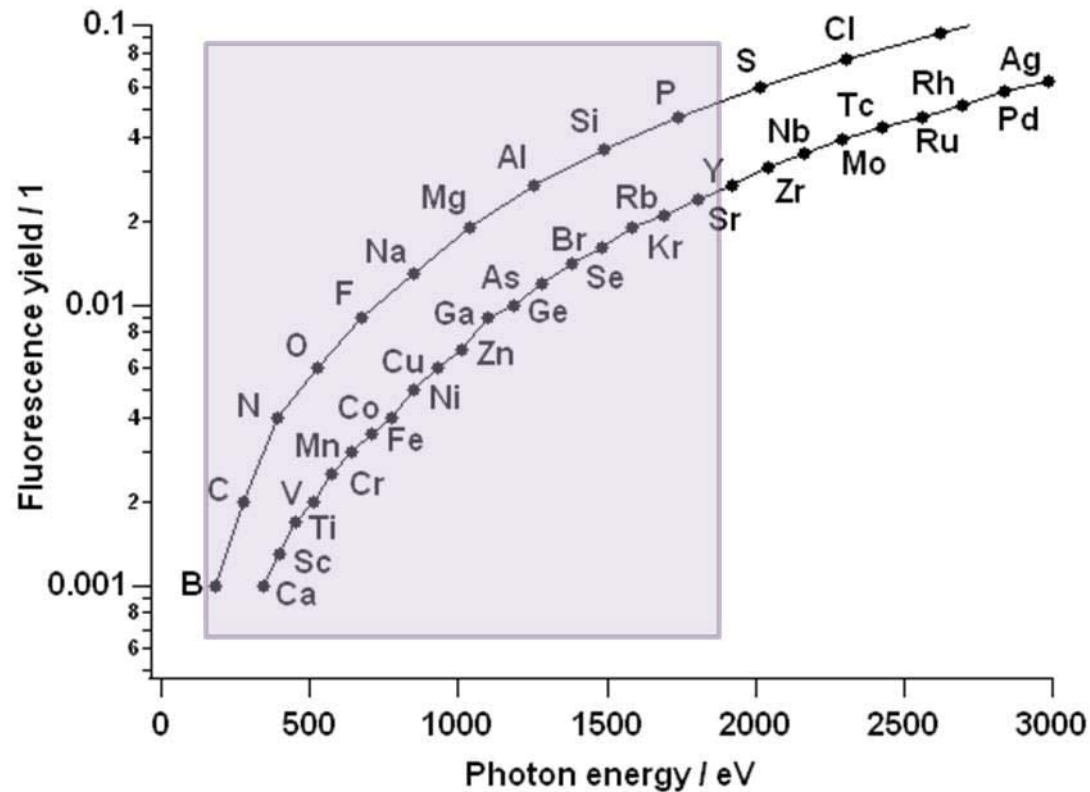


- Histogram coming from the multichannel analyser (ADC convertor)
 - Calibration with a known sample
 - Determination of chemical elements by using known tables (databases)
-



A novelty: Low-energy X-ray fluorescence

Simultaneous acquisition of absorption, differential phase contrast and LEXRF ?



Detecting trace elements:

X-ray fluorescence: **~1000x better sensitivity** than electrons for trace elemental mapping (ion concentrations etc.).
Parts per billion!

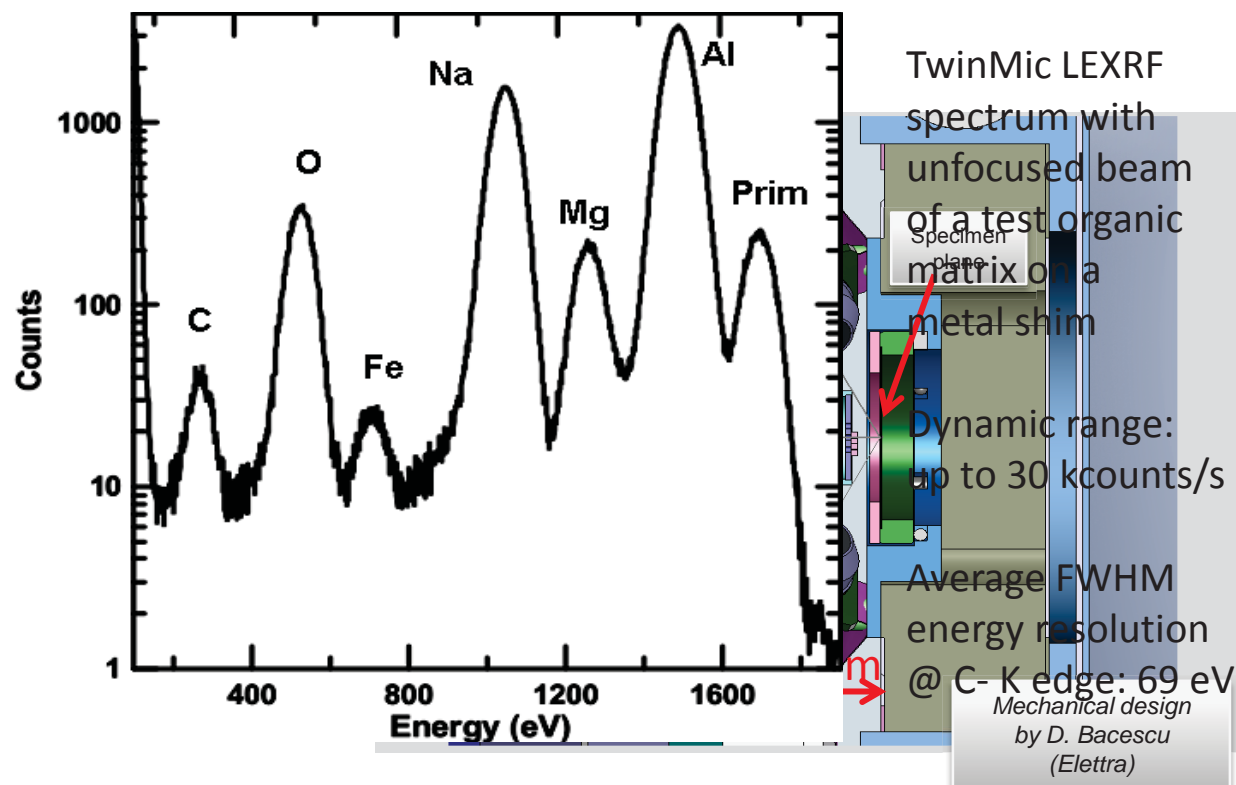
Low fluorescence yields for soft X-rays:

Is the signal sufficient for detecting trace elements in the ppm or ppb range?



A novelty: Low-energy X-ray fluorescence

Simultaneous acquisition of absorption, differential phase contrast and X-ray micro-fluorescence in STXM mode!



A. Longoni et al., Politecnico Milano/ INFN and ELETTRA

- Novel compact SDD technology
- Customized read-out electronics optimized to the TwinMic station
- Superior performance at low energies

Visualization of a Lost Painting by Vincent van Gogh Using Synchrotron Radiation Based X-ray Fluorescence Elemental Mapping

Joris Dik,^{*,†} Koen Janssens,[‡] Geert Van Der Snickt,[‡] Luuk van der Loeff,[§] Karen Rickers,^{||} and Marine Cotte^{†,⊗}

- Van Gogh (1853-1890) is one of the fathers of modern picture and was known for his vivid colors, the intense paint brushes dipinti and for his big productive career.
- His productivity is higher than we think since often he was re-utilising some older painting as base for a new painting.

Visible light



Radiography

IR Riflettografia

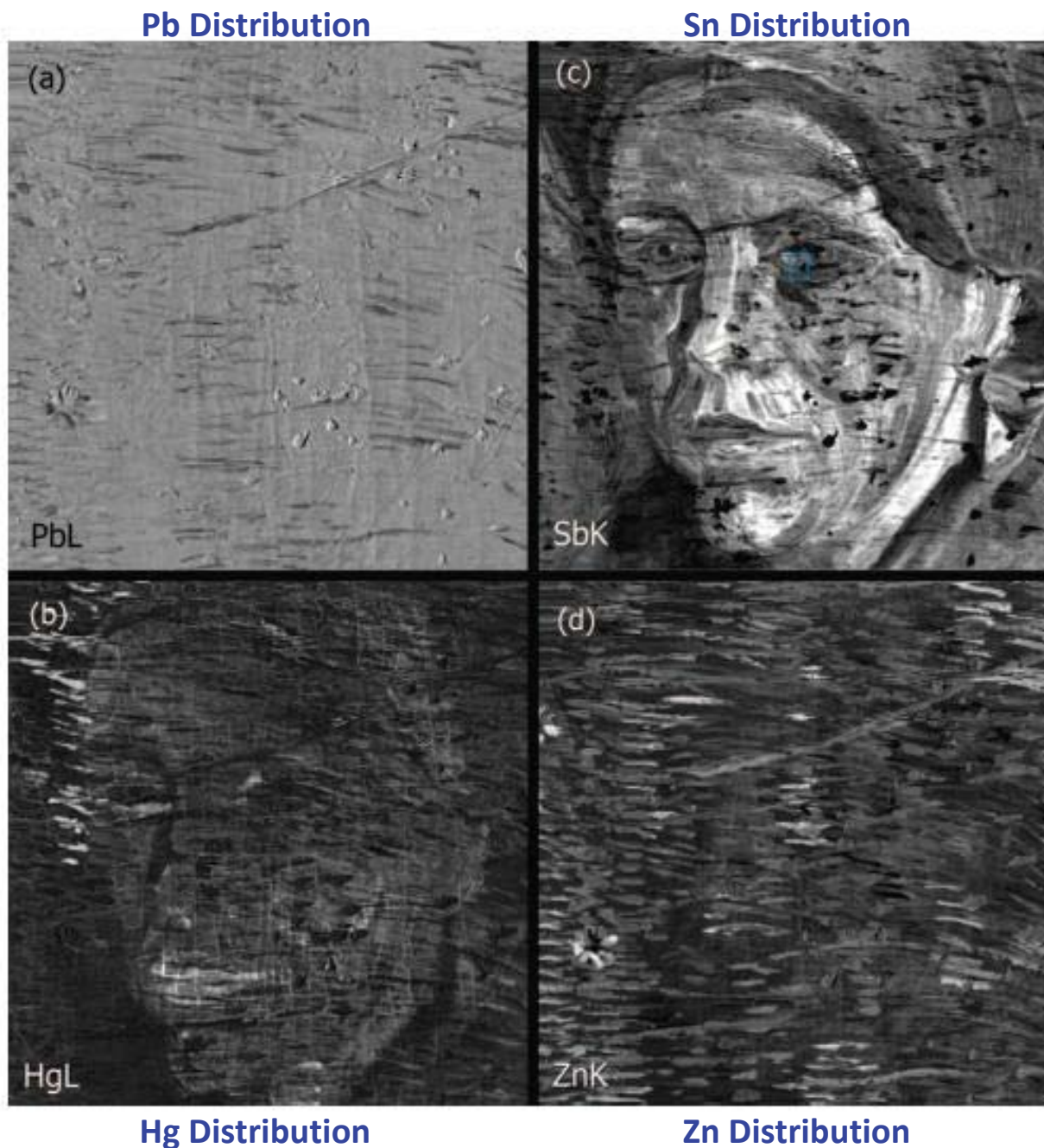
HASYLAB (Hamburg, Germany)

Beam ($0.5 \times 0.5 \text{ mm}^2$) at 38.5 keV

$17.5 \times 17.5 \text{ cm}^2$
dwell time: 2 s per pixel
total scan time ~ 2 days

The XRF scan revealed a number of elemental distributions that mostly correspond with the surface painting.

Its main elemental components include transition metals such as Mn, Cr, Co, Fe, Cu, Zn, As, and Ba.





(b) Detail from Head of a Woman, Nuenen, 1884-85, oil on canvas, 42 cm × 33 cm, Kröller-Müller Museum, Otterlo

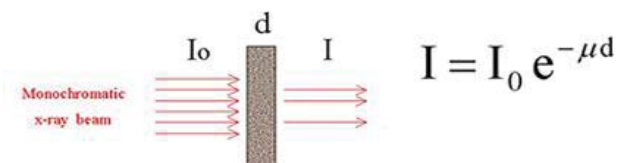
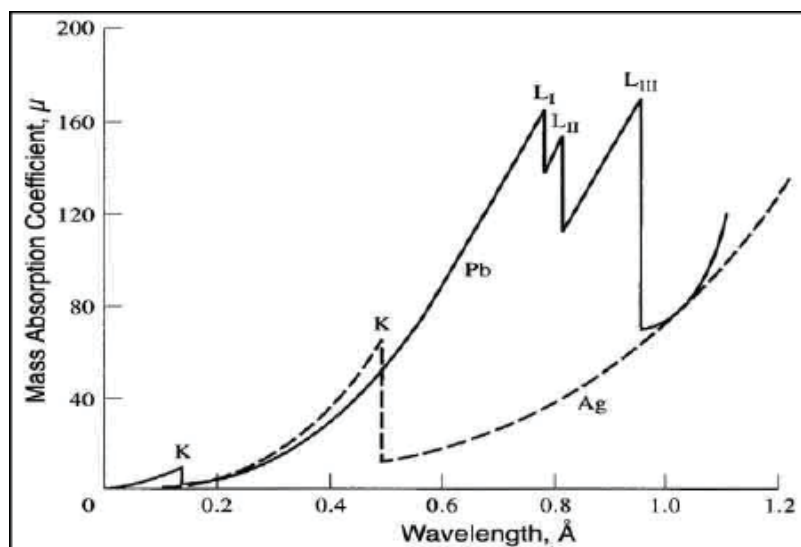
(c) Detail from Head of a Woman, Nuenen, winter 1884-85, oil on canvas, 42 cm × 34 cm, Van Gogh Museum, Amsterdam.

J Dik et al. "Visualization of a Lost Painting by Vincent van Gogh Using Synchrotron Radiation Based X-ray Fluorescence Elemental Mapping" *Anal. Chem.* 2008, 80, 6436–6442



X-ray Absorption Spectroscopy

- Element specific
- Applicable under extreme conditions (high-pressure, high temperature, in-situ)
- Applicable to gasses, liquids and solids
- Combination with microscopy



- The primary X-ray photons are absorbed when their energy is at least equal to the binding energy of the electrons.
- For lower energy the photons are easily transmitted by the sample
- When the X-ray photon reaches the electron binding energy absorption occurs
- By progressively increasing the energy the absorption efficiency decreases

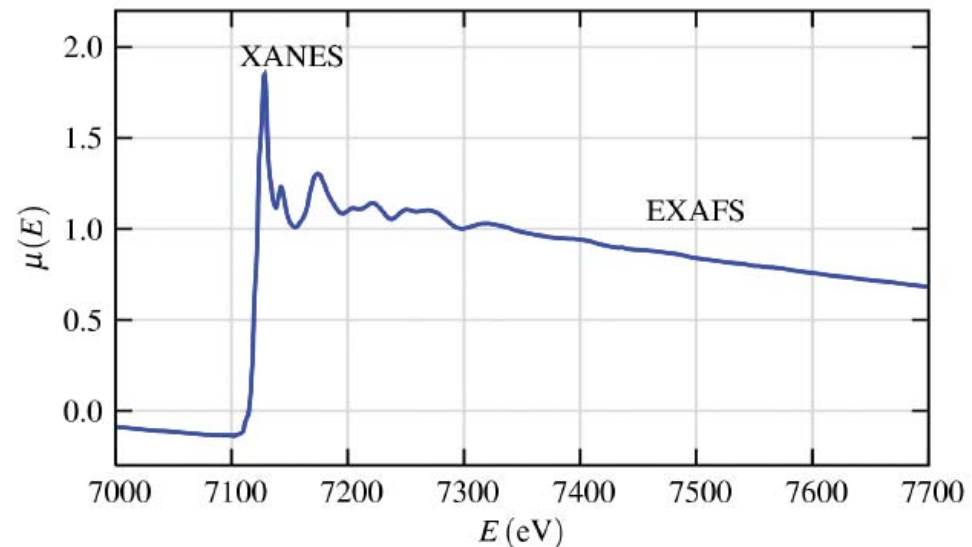


X-ray Absorption Fine Structure

- Spectroscopic technique
- Element-specific (x-rays are chosen to be at and above the binding energy of a particular core electronic level of a particular atomic species).
- XAFS can study elements with $Z > 15$ (all but the lightest elements have core-level binding energies in the x-ray regime).
- An energy-tunable x-ray source is needed to measure XAFS ([synchrotron](#)).
- The x-ray absorption spectrum is typically divided into two regimes: x-ray absorption near-edge spectroscopy (XANES) and extended x-ray absorption fine-structure spectroscopy (EXAFS).

XANES is strongly sensitive to formal oxidation state and coordination chemistry (e.g., octahedral, tetrahedral coordination) of the absorbing atom

EXAFS is used to determine the distances, coordination number, and species of the neighbors of the absorbing atom



XANES is region of x-ray absorption spectrum within ~ 50 eV of the absorption edge.

XANES on a paint sample

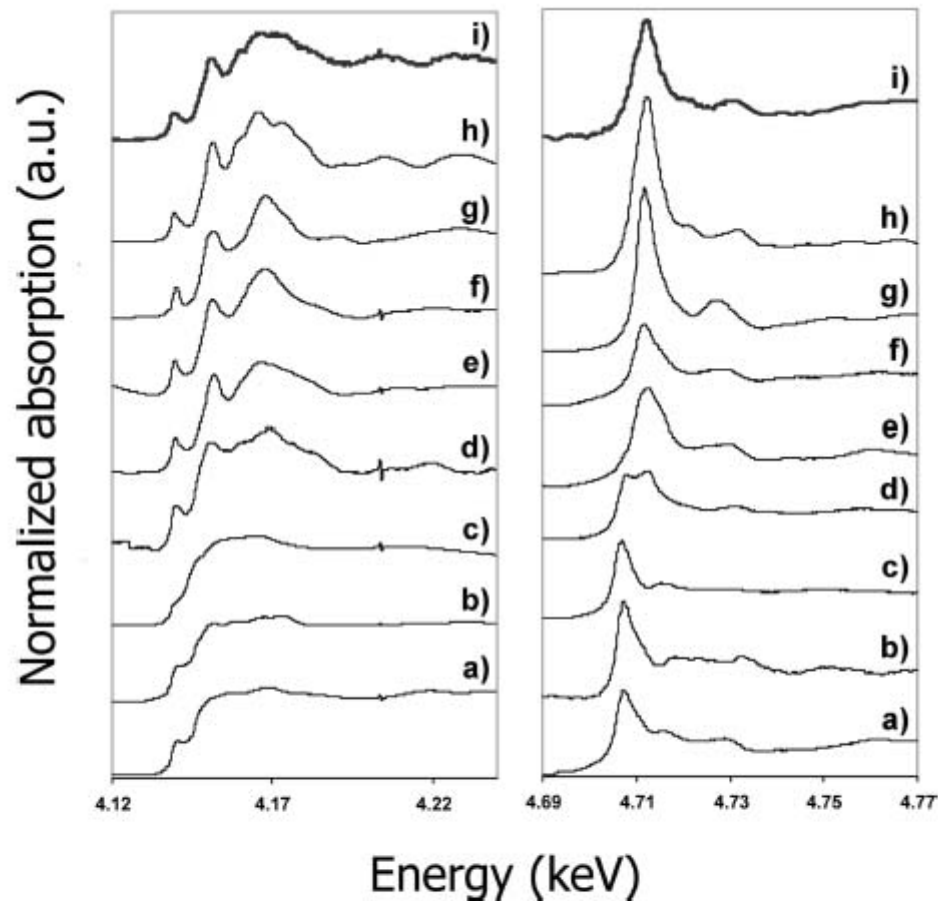


Figure 6. XANES spectra at the Sb-L_{III} edge (upper spectrum) and at the Sb-L_I edge (lower spectrum). Reference antimony compounds: Sb₂O₃ as (a) valentinite and as (b) senarmonite; (c) Sb₂S₂O, kermesite; (d) Sb₂O₄; (e) Sb₃O₆OH, stibiconite; (f) KSbO₃·3H₂O; (g) NaSbO₃OH·3H₂O; (h) Naples yellow; and (i) Sb pigment in the cross section of the Van Gogh painting (Figure 5).

the best agreement of spectra at the two L-edges corresponds to the Naples yellow spectra

(the same was verified on the K-edge directly on the painting)

STXM imaging coupled with XRF and XANES

Case study: **blackening of Pompeian Cinnabar Paintings** (M. Cotte, J. Susini, N. Metrich, A. Moscato, C. Gratziu, A. Bertagnini, M. Pagano "Blackening of Pompeian Cinnabar Paintings: X-ray Microspectroscopy Analysis", Anal. Chem. 2006, 78, 7484-7492.)

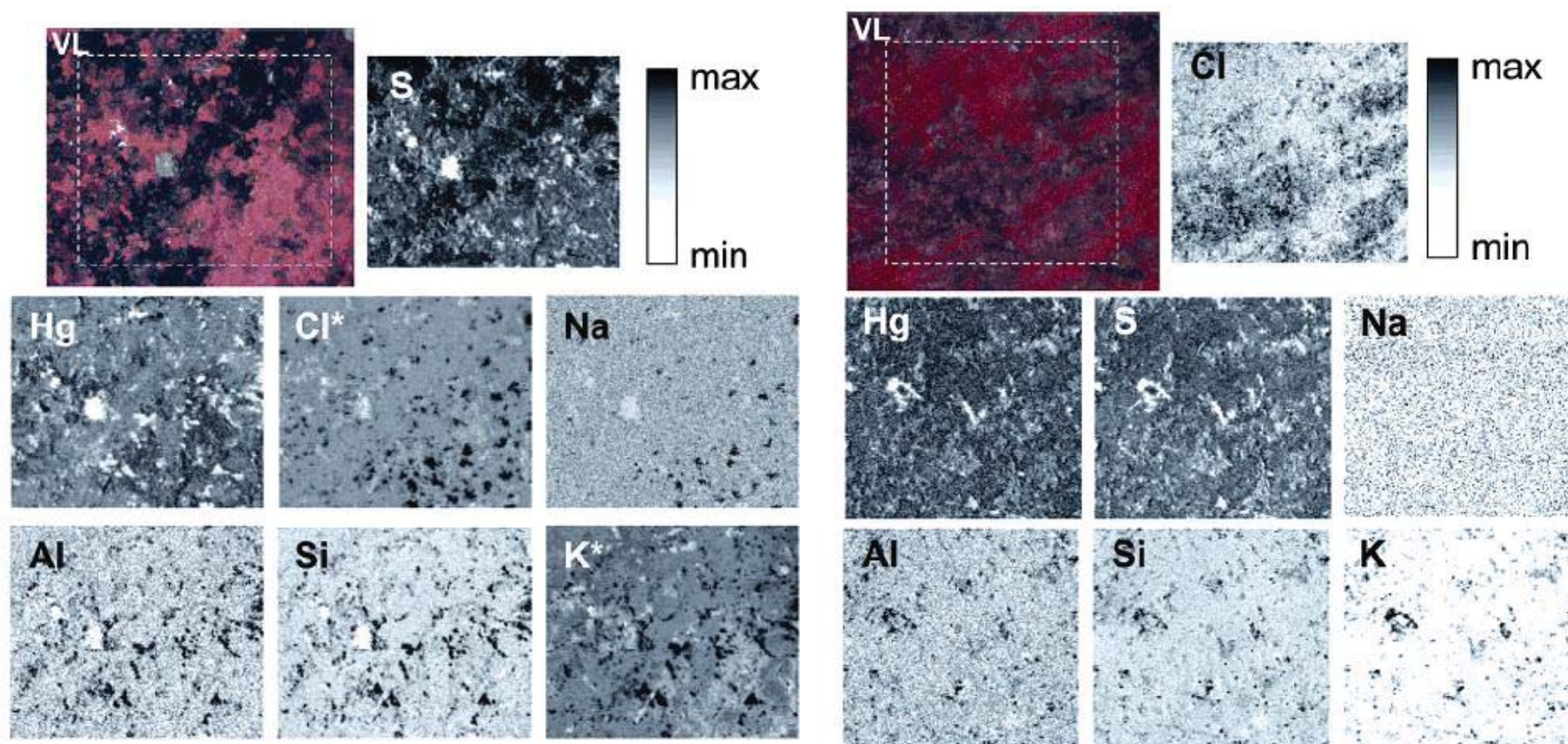
- The Pompeian red painting are suffering from degradation
- From the exavation (started in 1988 in Villa Sora) the vivid red painting started to darken progressively
- The darkening and degradation process is often attributed to the formation of black metacinnabar (through photoinduced conversion)

- Different samples with different degradation levels were selected
- Synchrhrotron radiation was used in order to have:
 - micro-spot
 - low detection limit
 - high chemical sensitivity

- X-ray microscopy
- XRF mapping to identify spatial distribution of chemical elements of interest
- XANES spectroscopy to probe local chemical speciation

STXM imaging coupled with XRF and XANES

XRF showed peculiar ditributon of Cl and S

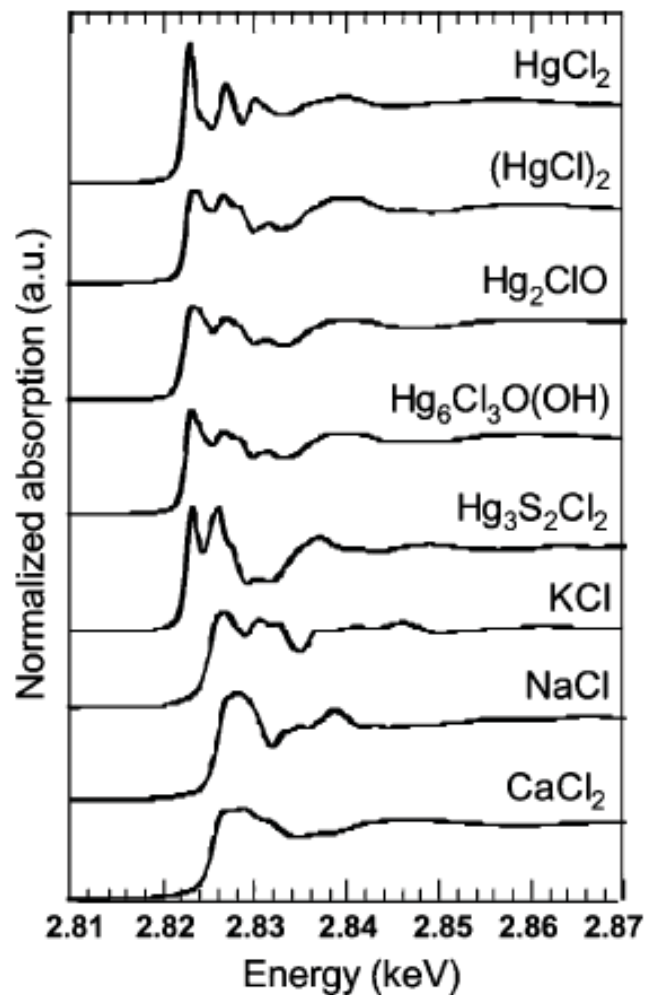


8mm x 7mm, pixel size 50x50 μm^2

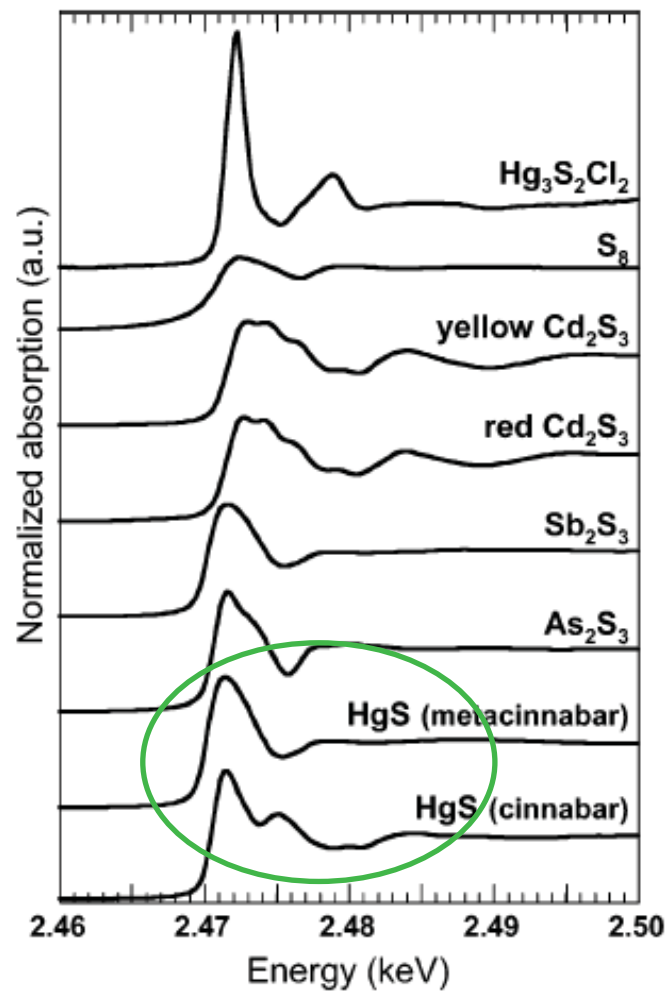
7mm x 7mm, pixel size 50x50 μm^2

STXM imaging coupled with XANES

Acquisition of reference compound spectra for calibration



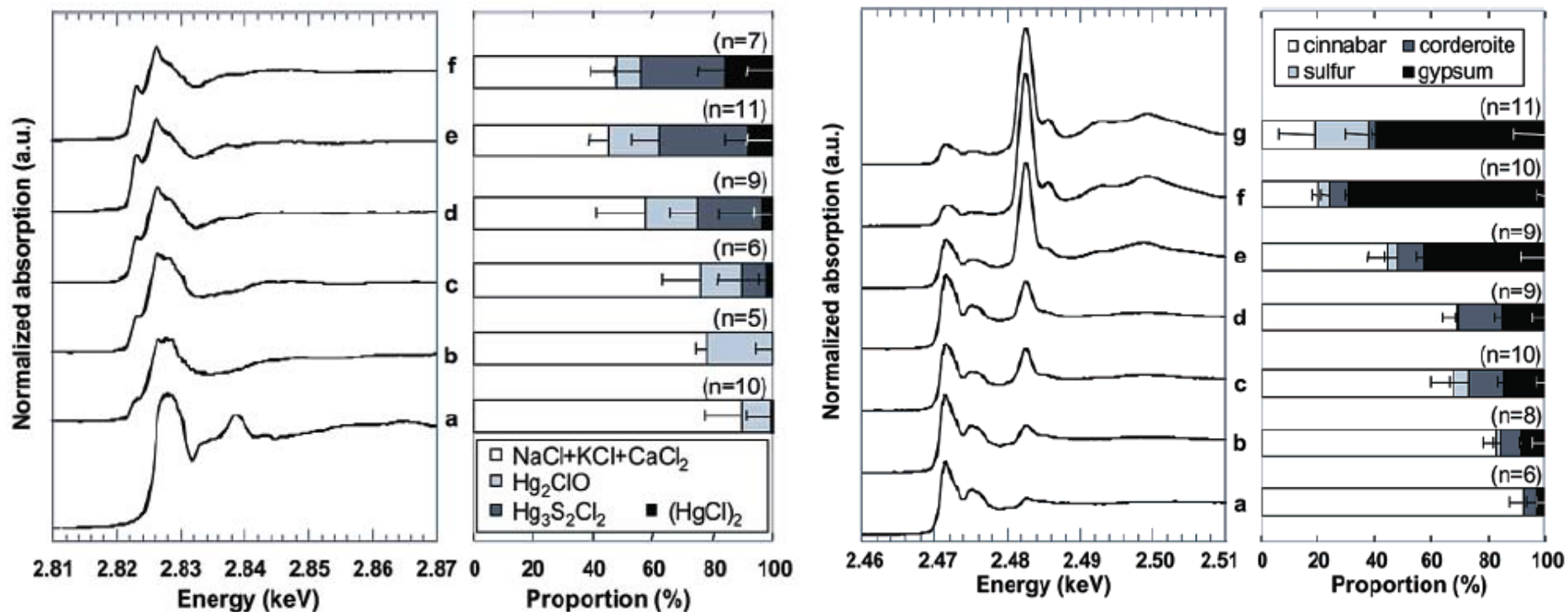
Chlorinated references



Sulfur references

STXM imaging coupled with XANES

By fitting the XAS with a linear combination of the reference compound spectra in order to identify the proportion of the different components in the altered zones



• Cl K-edge

In red and rust parts less than 20% of Hg is coordinated with Cl

In gray and black areas the Hg species are around 40-50%

• S K-edge

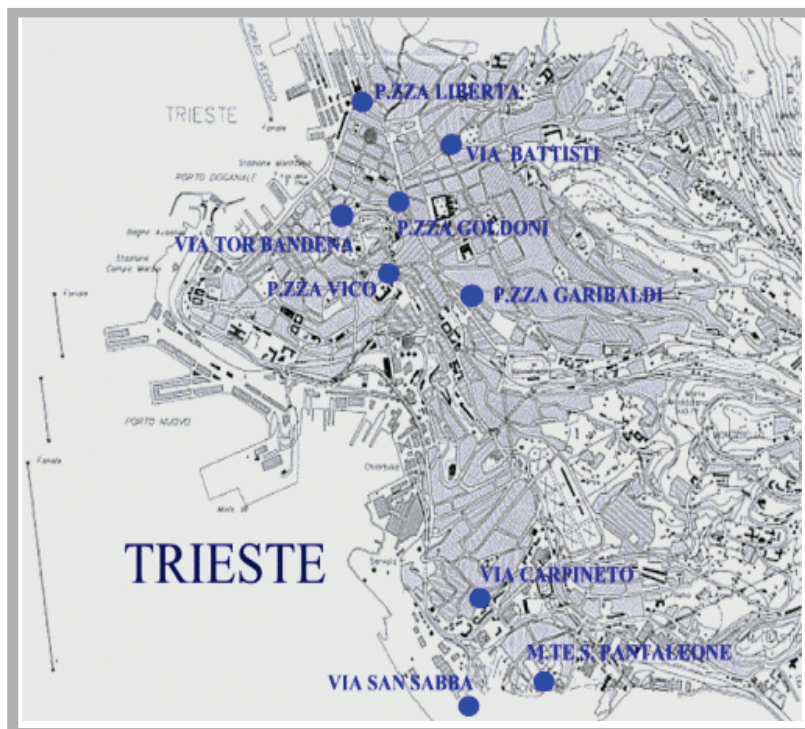
In one sample the amount of sulfate increases dramatically in dark areas (>50%)

In both samples high sulfate concentrations in white/orange spots

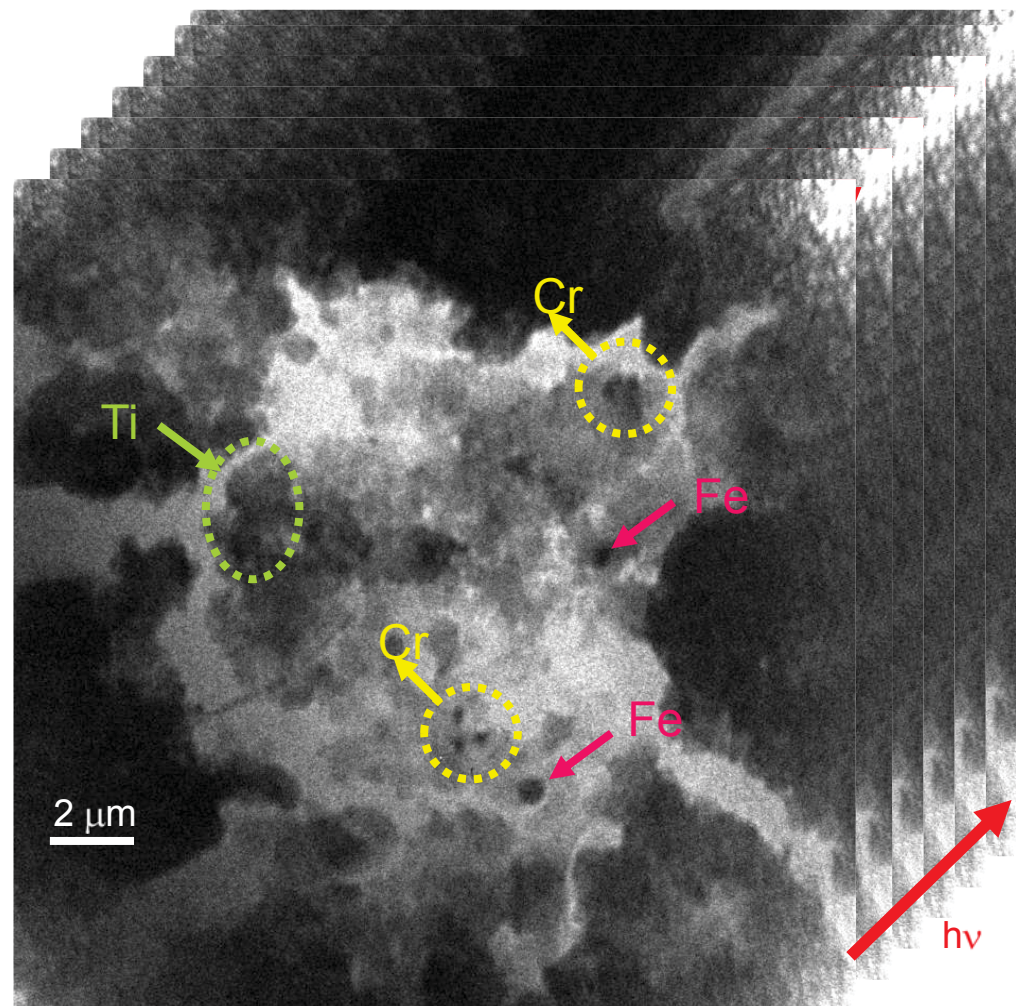
No contribution of metacinnabar



Environmental science: Analysis of air particulate matter

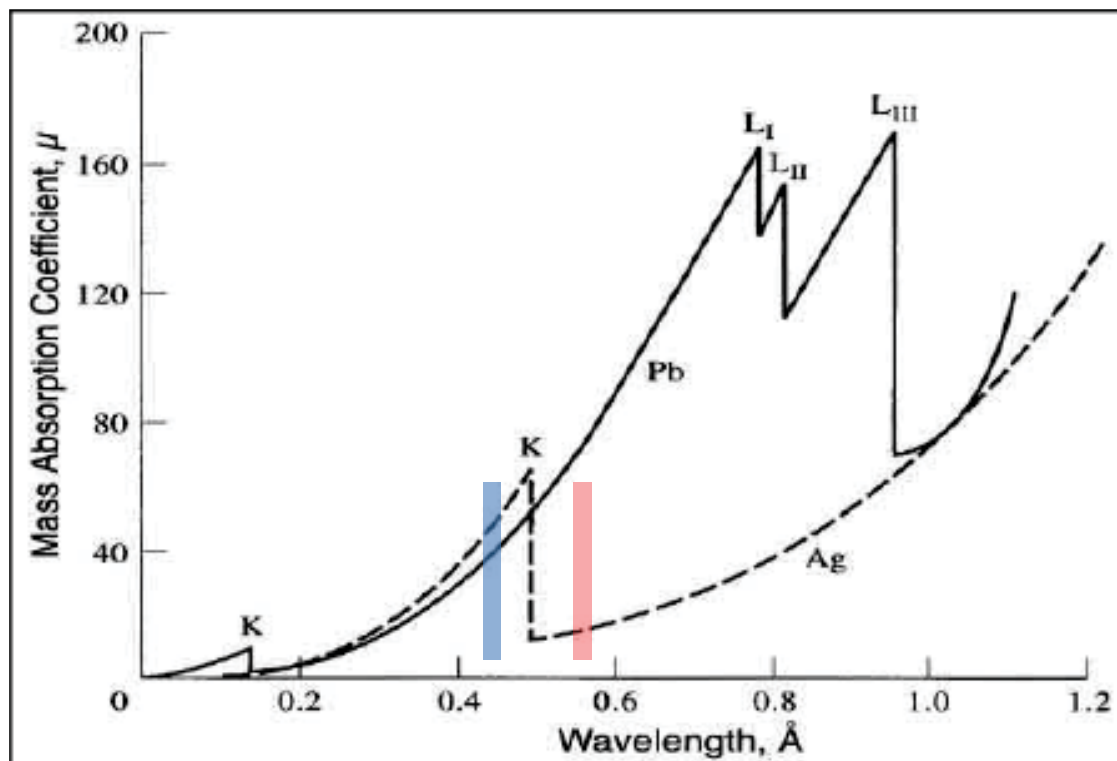


*P. Barbieri et al.,
Dept. of Chem., Univ. Trieste, I*





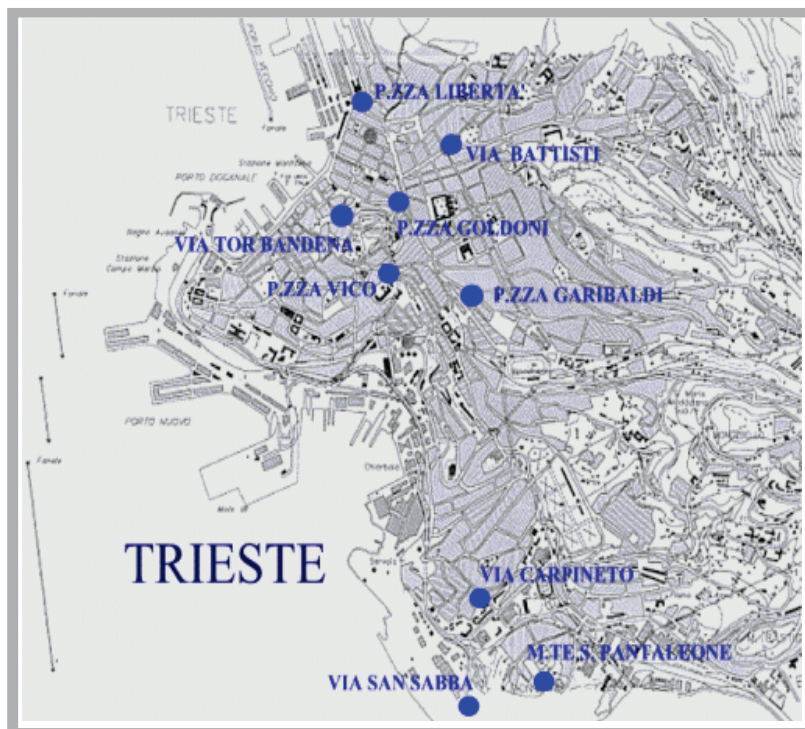
Across Edge Imaging



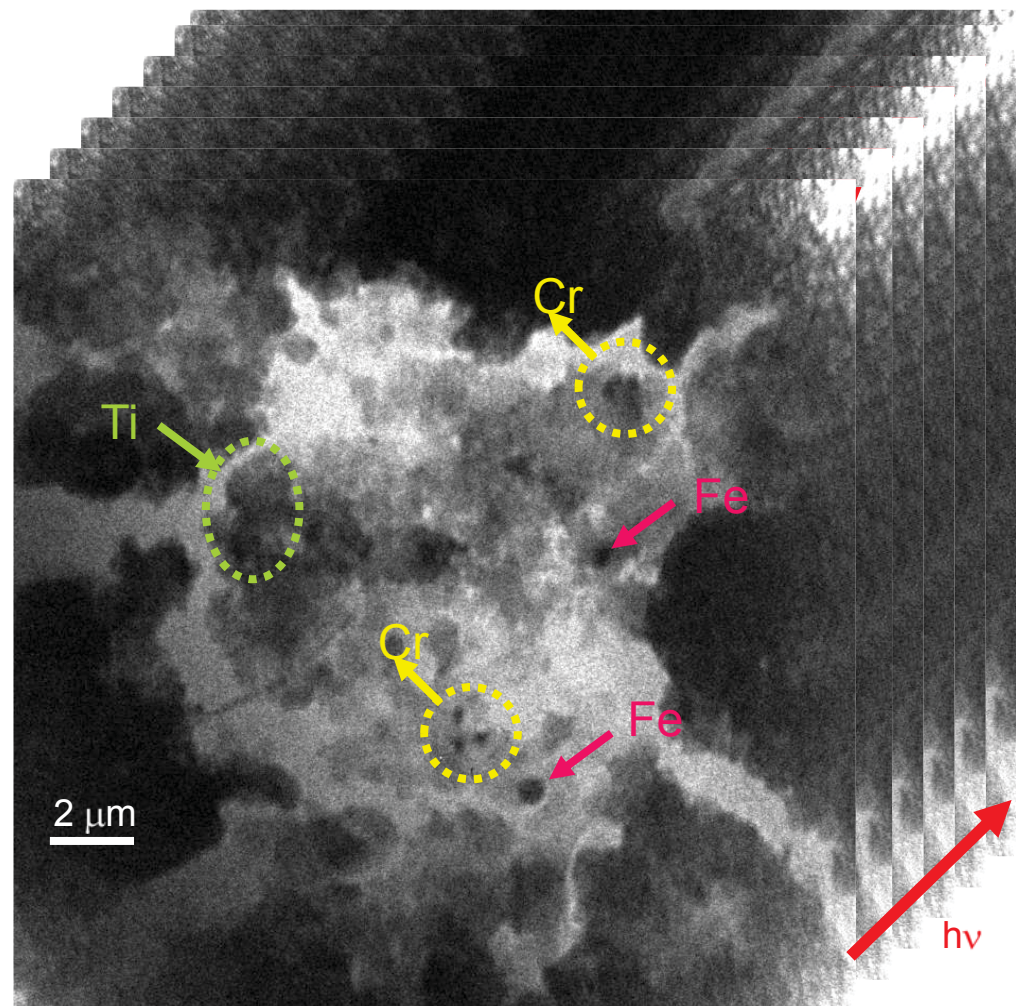
Acquisition of two images: Above and Below the K-edge



Environmental science: Analysis of air particulate matter

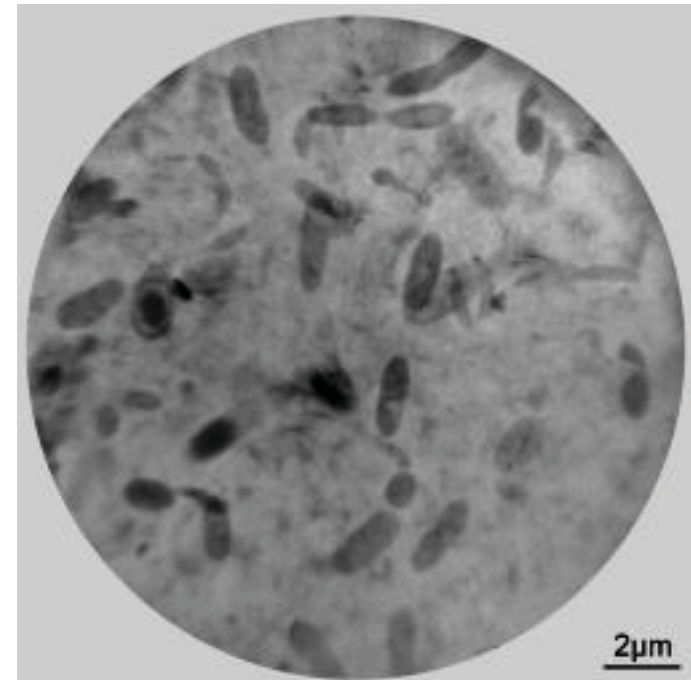
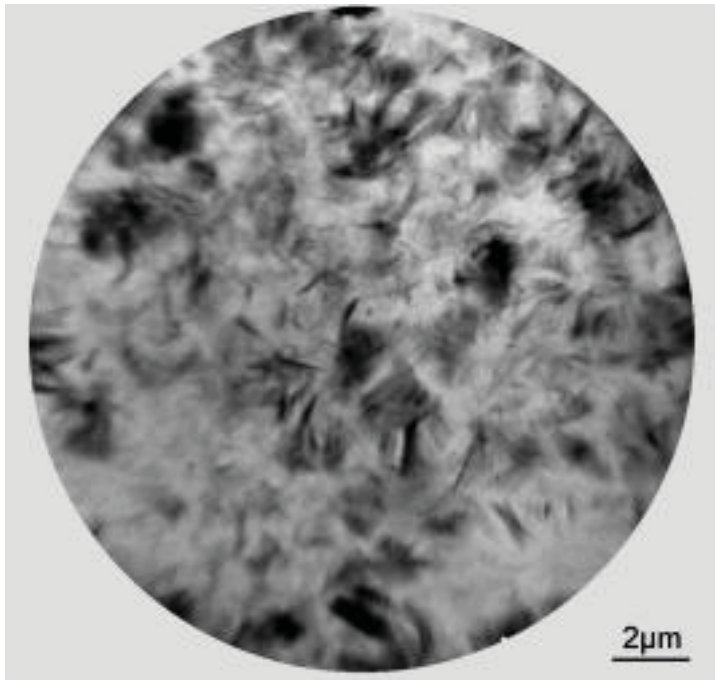


*P. Barbieri et al.,
Dept. of Chem., Univ. Trieste, I*



Environmental science: Imaging in liquids

Bacteria and clay dispersion: Destruction of associations of clay particles by soil microbes



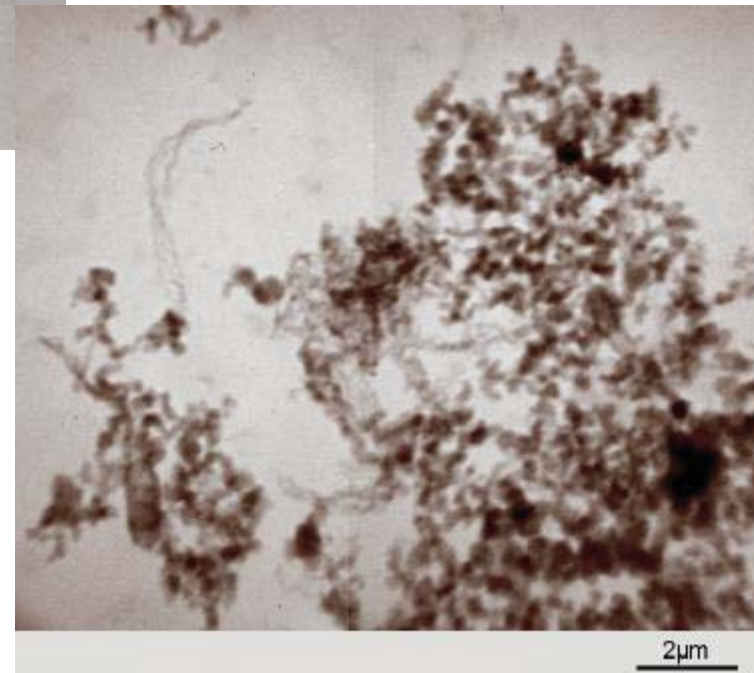
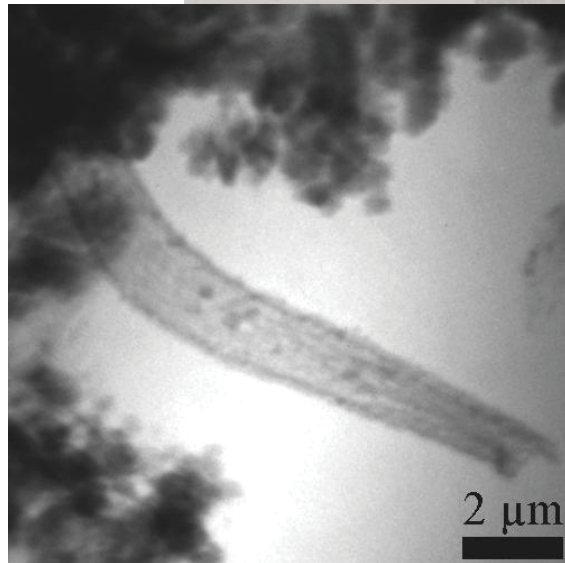
X-ray images acquired with the full-field imaging microscope at BESSY I @ 520 eV

J. Thieme et al., IRP, Uni Goettingen / G. Machulla, Uni Halle, D

Environmental science: Imaging in liquids



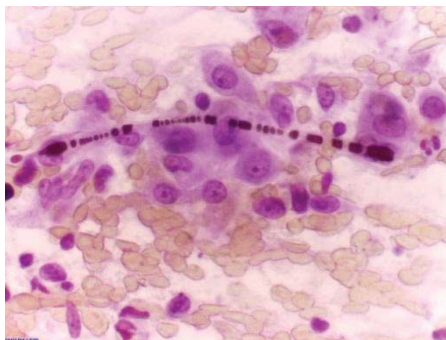
Iron precipitating bacteria:
Biological removal of Fe for
preparation of drinking water



J. Thieme et al., IRP, Uni Goettingen, D



Clinical medicine: Asbestos in lung tissue

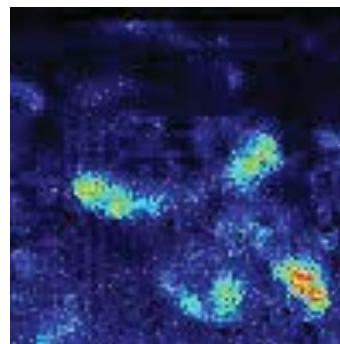


*M. Melato,
Monfalcone Hospital
L. Pascolo,
Sincrotrone Trieste*

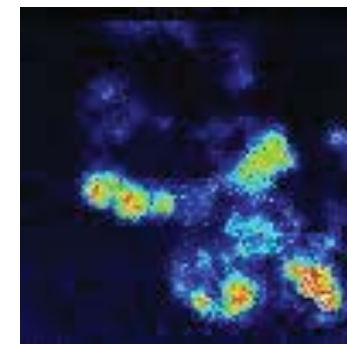
Cancer, death and
differentiation of lung
tissue due to asbestos



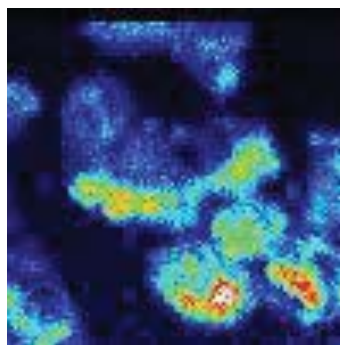
DPC



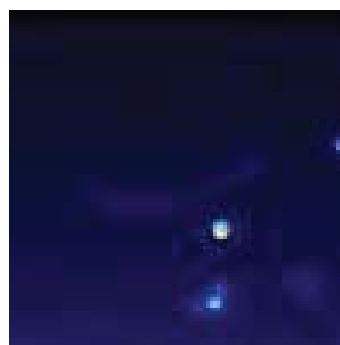
O



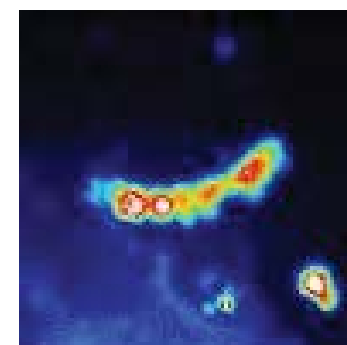
Fe



Mg



Al



Si

E=2019 eV, 50um x 50 um, 100 x 100 pixels

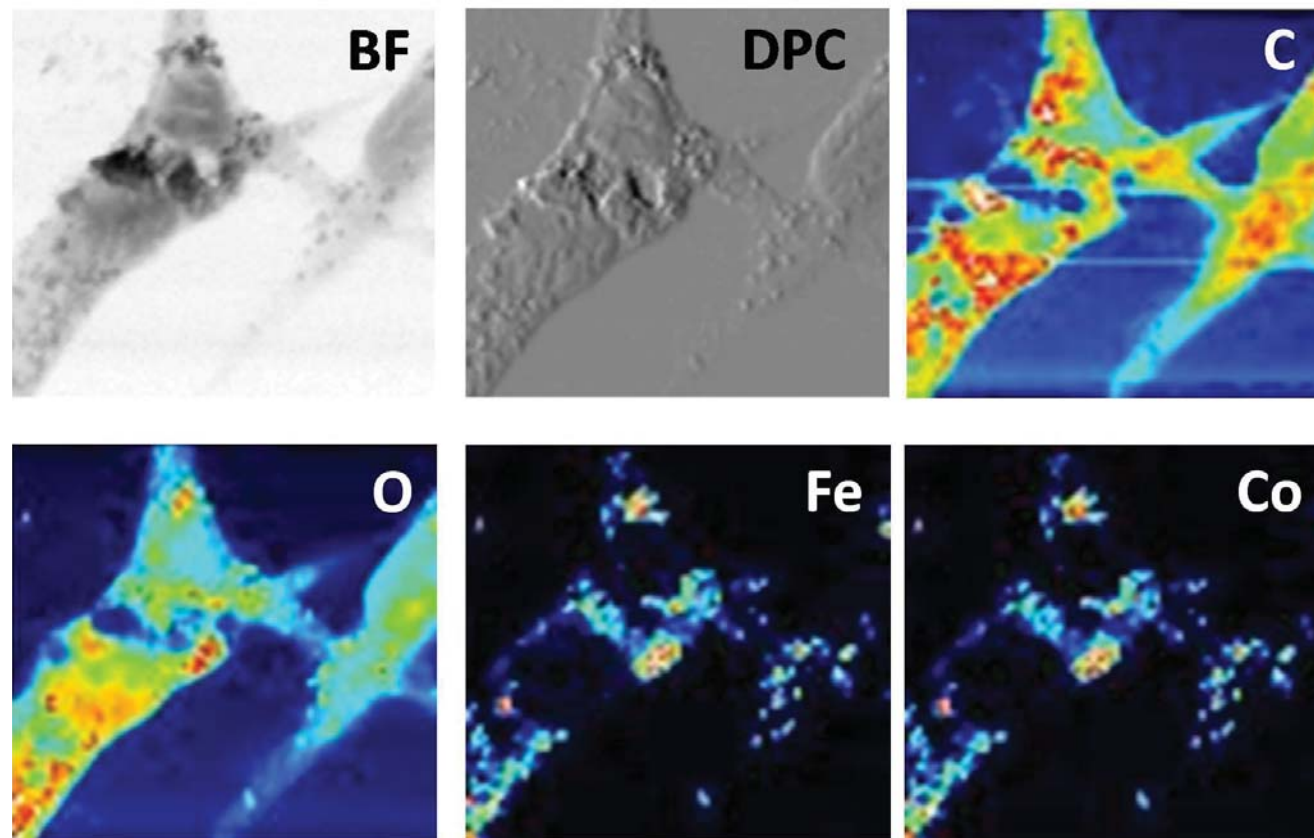


Nanotoxicology: CoFe_2O_4 ENPs



*G. Ceccone,
P. Marmorato, EC Joint
Research Center, Ispra, I*

Localization of
engineered nanoparticles
(ENPs) inside a cell and
on the possible effects on
the cell metabolic
behaviour



CoFe_2O_4 in mouse 3T3 fibroblast cells,
E=2019 eV, 25um x 35 um, 50 x 70 pixels, 15s/pixel

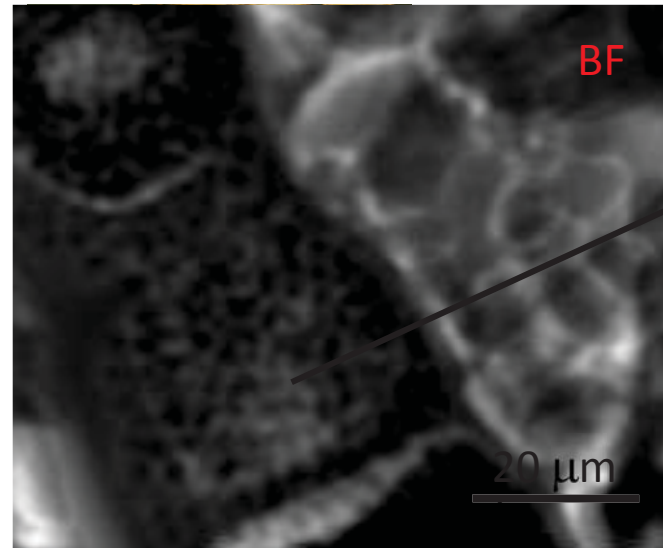


Biogenetics and Food Science: Inside the wheat

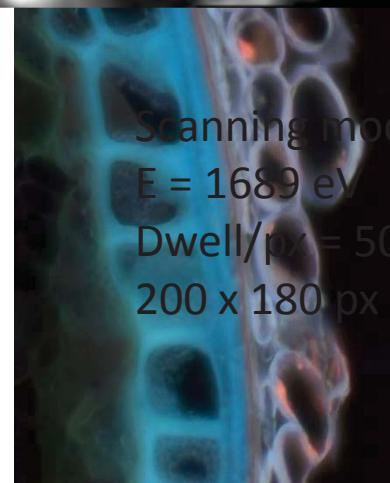
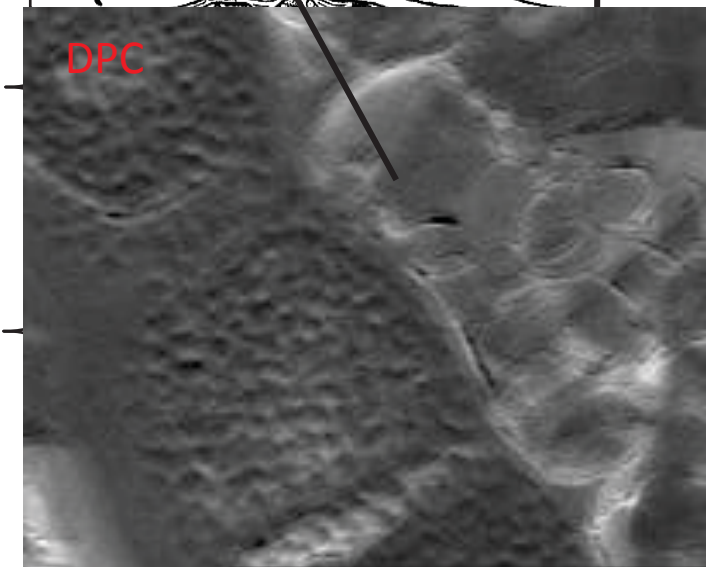
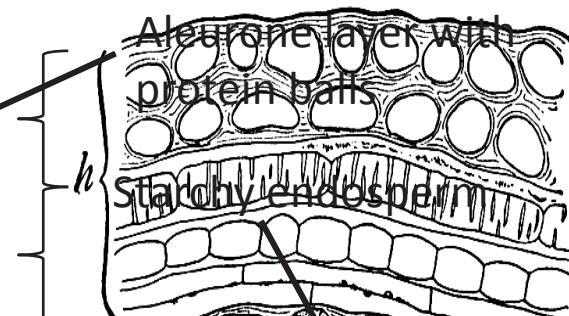


*Ivan Kreft,
University Ljubljana*

Functionality and toxicity of Zn in wheat and buckwheat analyzed on sub-cellular level



Structure of a wheat grain



Scanning mode:
E = 1689 eV
Dwell/px = 50 ms
200 x 180 px
Endosperm with starch granules



Biogenetics and Food Science: Inside the wheat



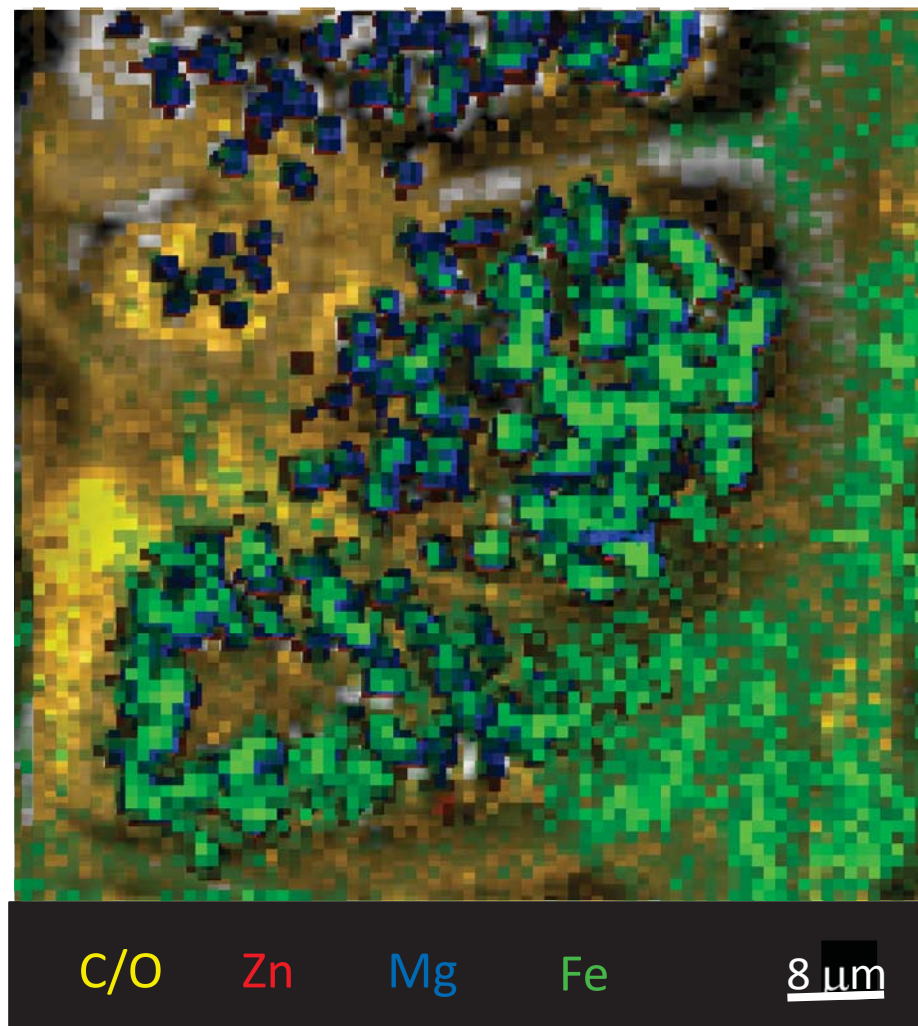
*Ivan Kreft,
Fac. of Biotechnology,
University Ljubljana*

Functionality and toxicity of Zn in wheat and buckwheat analyzed on sub-cellular level

Healthy control wheat

E=1686 eV
80 x 80 μm^2
80 x 80 px
8 s dwell/ px
1 μm resolution
4 detectors
New STXM optic

*Specimen preparation
by Paula Pongrac and
Katharina Vogel,
Uni Ljubljana, Slo*





Biotechnology: Al in tea leaves

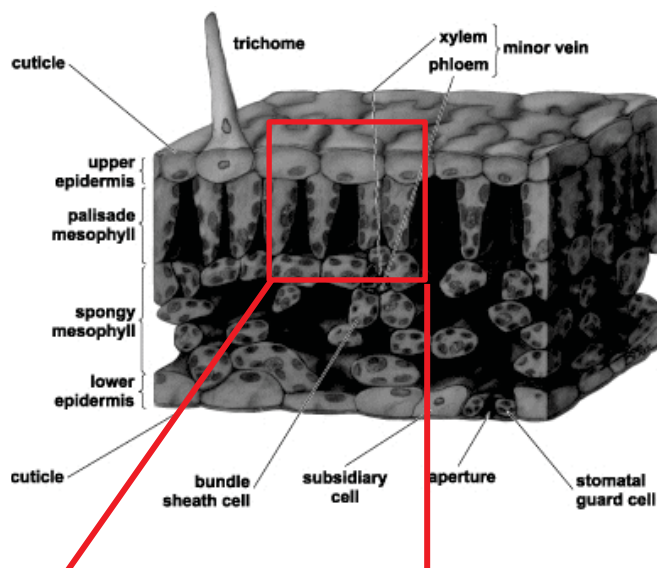


*C. Poschenrieder,
Uni Barcelona, ES*

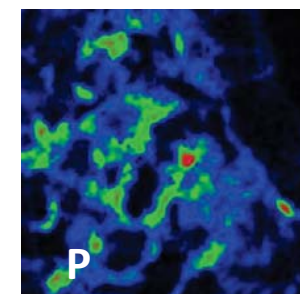
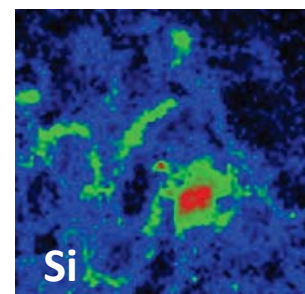
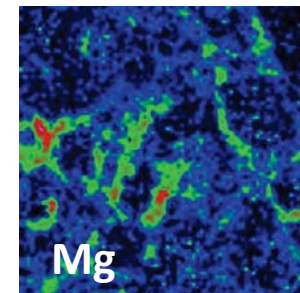
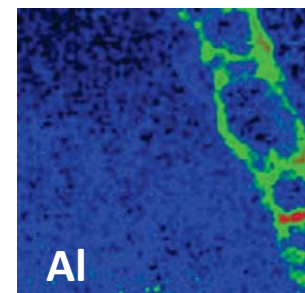
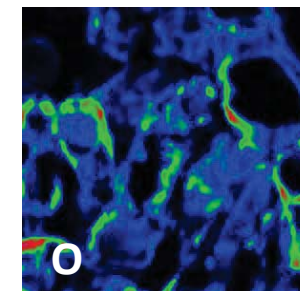
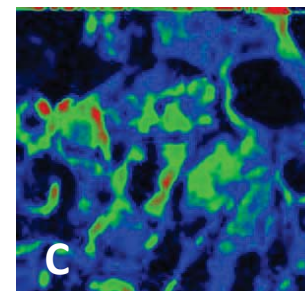
*Katharina. Vogel,
University Ljubljana, SI*

Functionality and
toxicity of Al in
tea leaves
analyzed on sub-
cellular level

Cross-section of a leaf



E=2.19 keV
80 x 80 μm^2
80 x 80 px
12s /px





Phytoremediation

- **Phytoremediation** consists of mitigating pollutant concentrations in contaminated soil, water or air by means of plants able to contain, degrade, or eliminate metals, pesticides, solvents, explosives, crude oil and its derivatives
- Phytoremediation is an emerging technology that employs the use of plants for the clean-up of contaminated environments.
- Progress in the field is however handicapped by limited knowledge of the biological processes involved in plant metal uptake, translocation, tolerance and plant–microbe–soil interactions
- A better understanding of the basic biological mechanisms involved in plant/microbe/soil/contaminant interactions would allow further optimization of phytoremediation technologies



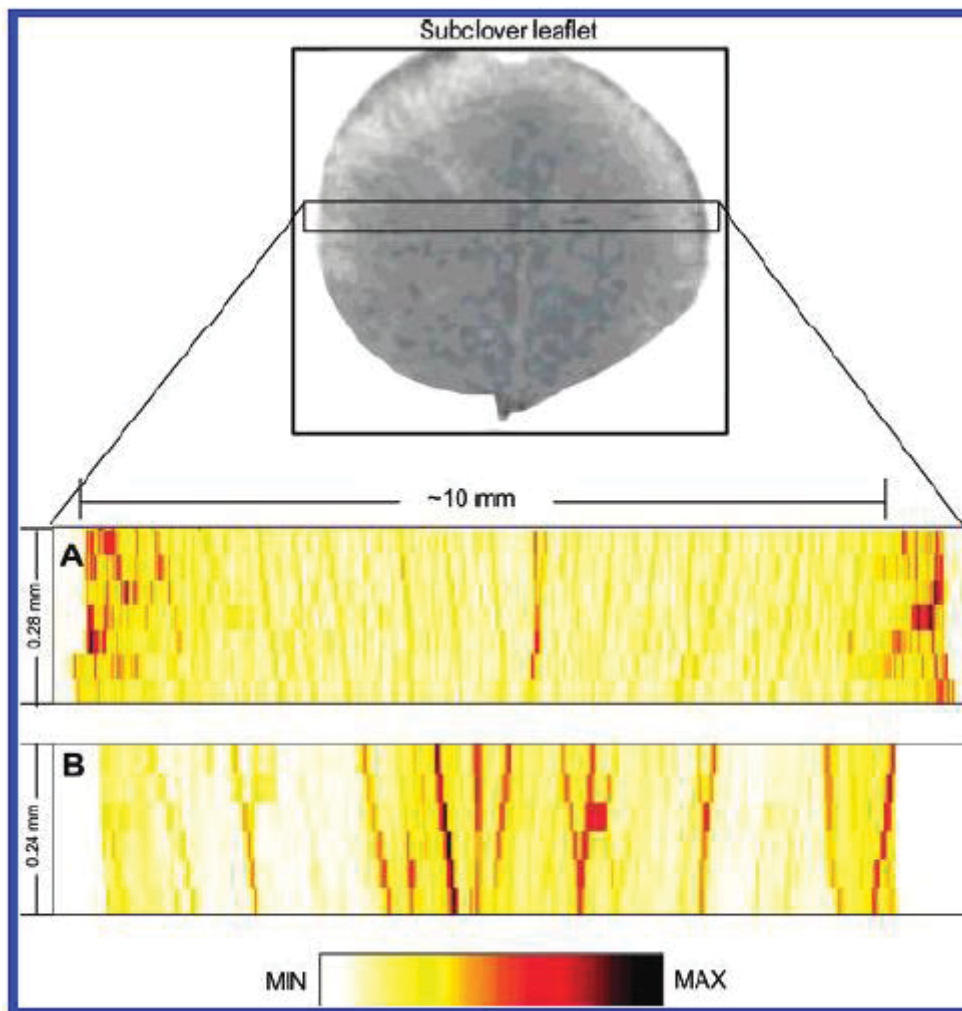
Localization and Speciation of Chromium in Subterranean Clover

- In order to optimize of phytoremediation as a potential remediation strategy and to assess potential health hazards with this process, it is helpful to understand the mechanisms of Cr uptake, translocation, tolerance, and bonding by plants and the conditions under which Cr is maximally absorbed and/or immobilized.
- The oxidation state of Cr significantly affects its absorption and translocation by plants.
- SXRF microprobe spectroscopy was used to localize Cr in the leaf
- XANES spectroscopy was used to determine the oxidation state of Cr
- XRF and XANES experiments performed at the National Synchrotron Light Source (NSLS), Brookhaven National Laboratory, NY, beamline X-26A



XRF spectroscopy

Beam size:
10 μ m x 12 μ m



Leaves of plants
grown in 0.04 mmol
Cr(VI) L⁻¹ for 21 days

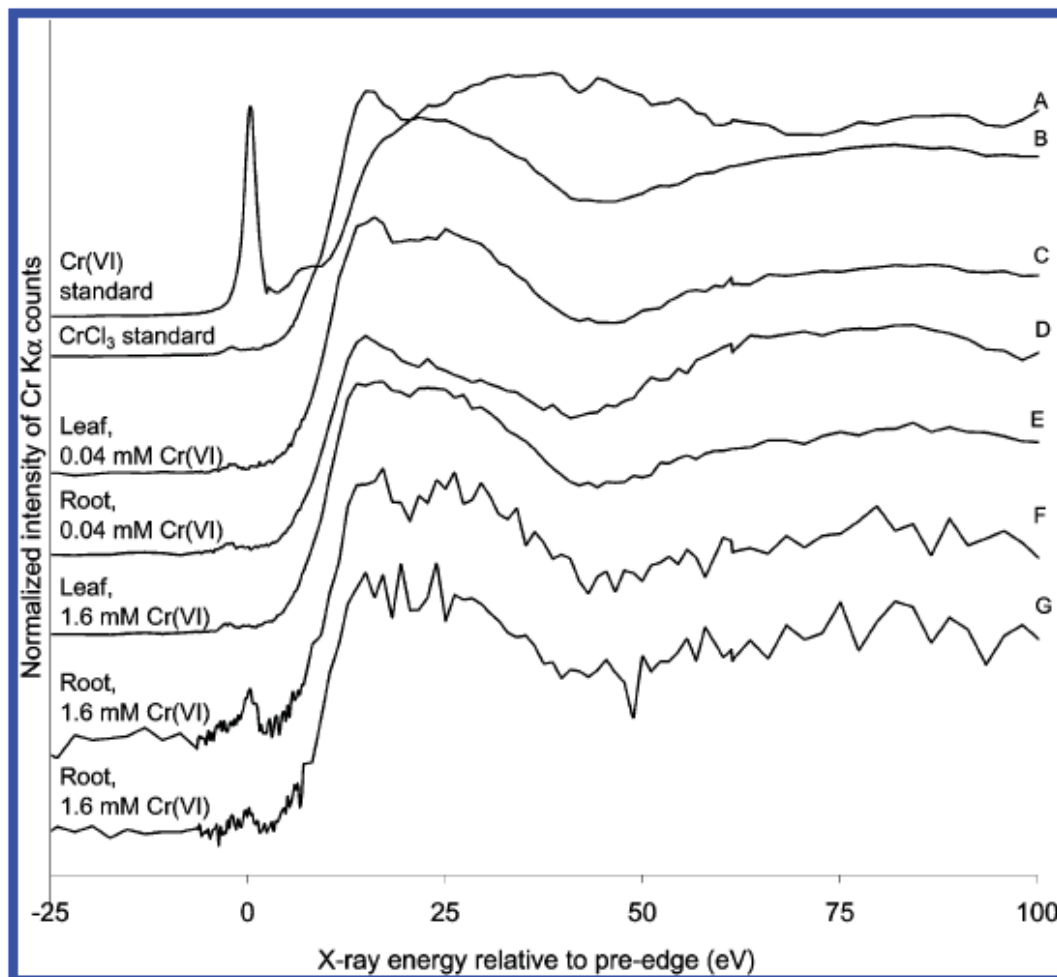
Accumulation Cr at the leaf
margins and slightly elevated
concentrations in the veins

Leaves of plants
grown in 1.6 mmol
Cr(VI) L⁻¹ for 4 days

Highest levels of Cr at the veins,
with only slight accumulations at
the leaf margins and in areas
surrounding the midvein



XANES spectroscopy



XANES spectra of 5% (w/w) standards of Cr(VI) and Cr(III) and fresh tissue from subclover plants grown with 0.04 and 1.6 mmol Cr(VI) L⁻¹. Spectra F and G are successive scans at the same position on the root.



XRF and XANES results

- The visual symptom of Cr toxicity of subclover plants grown in 1.6mmolCr(VI) L⁻¹ for 4 days was distinctly different from that at the lower concentration of Cr(VI).
 - Plant death occurred within 7-10 days after initiation of the Cr(VI) treatment. The higher concentrations of Cr(VI) apparently interfered with transport processes, which might have contributed to plant death.
 - XANES: relatively rapid reduction of Cr(VI), which continued following excision of the tissue from the plant. The **influence of the X-ray beam** on the reduction of Cr(VI) is not known and also might have contributed to the observed reduction of Cr(VI).
 - XANES: reduction of Cr(VI) to Cr(III) occurred in or on the roots of subclover plants grown in Cr(VI).
 - **Low treatment concentrations** of Cr(VI): the plant appears to have been able to quantitatively reduce Cr(VI) to Cr(III).
 - **Higher concentrations**: some of the Cr(VI) is still present in the roots. The reduction of Cr(VI) to Cr(III) is an important mechanism of detoxification by the plant.
-



Conclusions

- **Synchrotron radiation offers a big range of analytical techniques for material analysis**
 - **SR offers higher brightness (shorter acquisition time, more sample analysed, better statistics...) and collimated beams**
 - **But limited access to users**
 - **X-ray microscopy with simultaneous acquisition of absorption, phase contrast can be a powerful complementary tool to traditional techniques, especially when combined with XRF and XANES spectroscopies**
 - **XRF analysis can provide useful information related to the distribution of the chemical elements**
 - **XANES spectroscopy combined with X-ray microscopy allows identifying oxidation states of chemical elements**
 - **Suitable sample preparation is crucial**
-